GRAVITATIONAL WAVES: A NEW WINDOW TO EXPLORE THE UNIVERSE

Philippe Jetzer

Universität Zürich

Madrid, 15 December 2017

Gravitational Waves

2 December 1915:
Einstein completes General Relativity
(A. Einstein,
Sitz. Ber. Preuss. Akad. Wiss. Berlin,

- December 1915, 844-847)

June 1916:
Gravitational Waves are predicted
(A. Einstein,
Sitz. Ber. Preuss. Akad. Wiss. Berlin,

- June 1916, 688-696
- January 1918, 154-167)

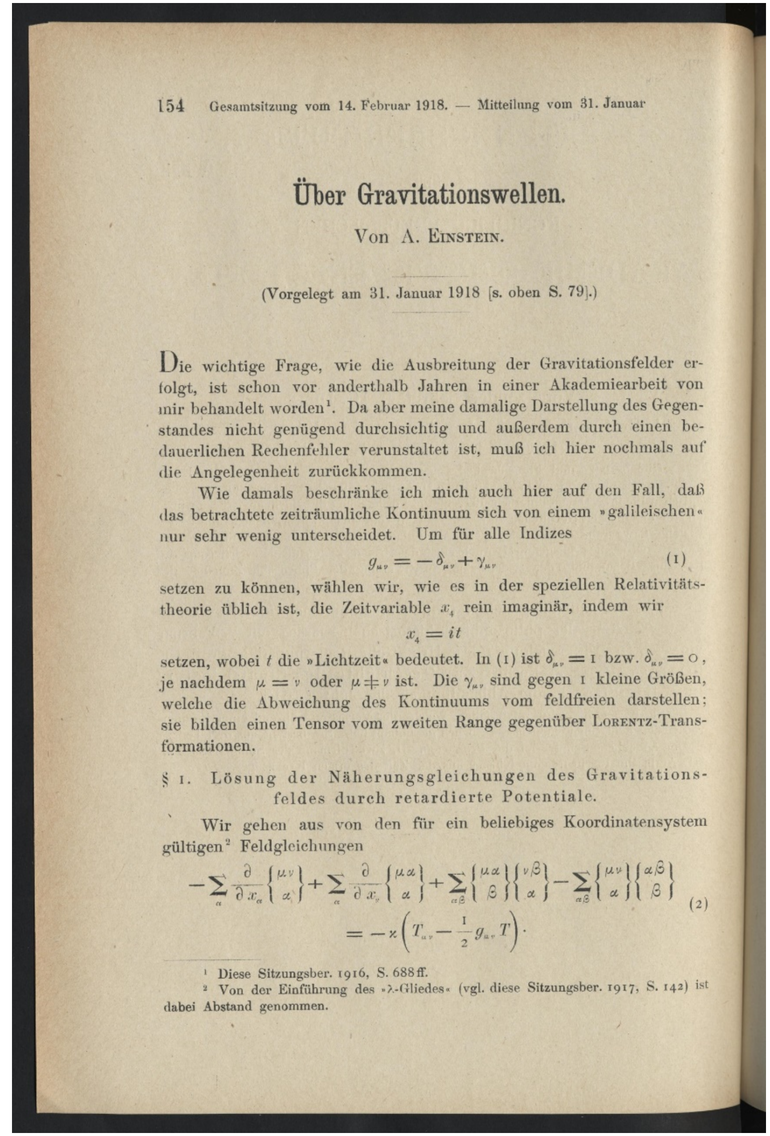

154 Gesamtsitzung vom 14. Februar 1918. — Mitteilung vom 31. Januar

Über Gravitationswellen.

Von A. Einstein.

(Vorgelegt am 31. Januar 1918 [s. oben S. 79].)

Die wichtige Frage, wie die Ausbreitung der Gravitationsfelder erfolgt, ist schon vor anderthalb Jahren in einer Akademiearbeit von mir behandelt worden[1]. Da aber meine damalige Darstellung des Gegenstandes nicht genügend durchsichtig und außerdem durch einen bedauerlichen Rechenfehler verunstaltet ist, muß ich hier nochmals auf die Angelegenheit zurückkommen.

Wie damals beschränke ich mich auch hier auf den Fall, daß das betrachtete zeiträumliche Kontinuum sich von einem »galileischen« nur sehr wenig unterscheidet. Um für alle Indizes

$$g_{\mu\nu} = -\delta_{\mu\nu} + \gamma_{\mu\nu} \qquad (1)$$

setzen zu können, wählen wir, wie es in der speziellen Relativitätstheorie üblich ist, die Zeitvariable x_4 rein imaginär, indem wir

$$x_4 = it$$

setzen, wobei t die »Lichtzeit« bedeutet. In (1) ist $\delta_{\mu\nu} = 1$ bzw. $\delta_{\mu\nu} = 0$, je nachdem $\mu = \nu$ oder $\mu \neq \nu$ ist. Die $\gamma_{\mu\nu}$ sind gegen 1 kleine Größen, welche die Abweichung des Kontinuums vom feldfreien darstellen; sie bilden einen Tensor vom zweiten Range gegenüber Lorentz-Transformationen.

§ 1. Lösung der Näherungsgleichungen des Gravitationsfeldes durch retardierte Potentiale.

Wir gehen aus von den für ein beliebiges Koordinatensystem gültigen[2] Feldgleichungen

$$-\sum_\alpha \frac{\partial}{\partial x_\alpha}\begin{Bmatrix}\mu\nu\\\alpha\end{Bmatrix} + \sum_\alpha \frac{\partial}{\partial x_\nu}\begin{Bmatrix}\mu\alpha\\\alpha\end{Bmatrix} + \sum_{\alpha\beta}\begin{Bmatrix}\mu\alpha\\\beta\end{Bmatrix}\begin{Bmatrix}\nu\beta\\\alpha\end{Bmatrix} - \sum_{\alpha\beta}\begin{Bmatrix}\mu\nu\\\alpha\end{Bmatrix}\begin{Bmatrix}\alpha\beta\\\beta\end{Bmatrix} = -\varkappa\left(T_{\mu\nu} - \frac{1}{2}g_{\mu\nu}T\right). \qquad (2)$$

[1] Diese Sitzungsber. 1916, S. 688ff.

[2] Von der Einführung des »λ-Gliedes« (vgl. diese Sitzungsber. 1917, S. 142) ist dabei Abstand genommen.

Gravitational Waves

Gravitational waves are solutions of the linearized Einstein Field Equations:

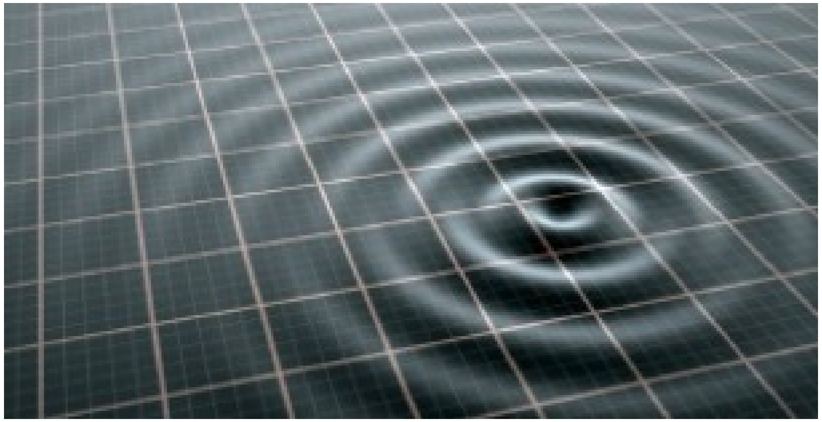

$$g_{\mu\nu} = \eta_{\mu\nu} + h_{\mu\nu} \quad \text{with} \quad |h_{\mu\nu}| \ll 1$$

$$G\left[g_{\mu\nu}\right] = \Box h_{\mu\nu} = 0\,, \qquad \Box = \nabla^2 - \frac{1}{c^2}\partial_t^2$$

Understanding Gravitational Waves

- Strong analogies with EM radiation
  - Two transverse polarisations
  - Move at the speed of light, follow geometrical optics
  - Same behaviour with gravitational lensing, cosmological redshift

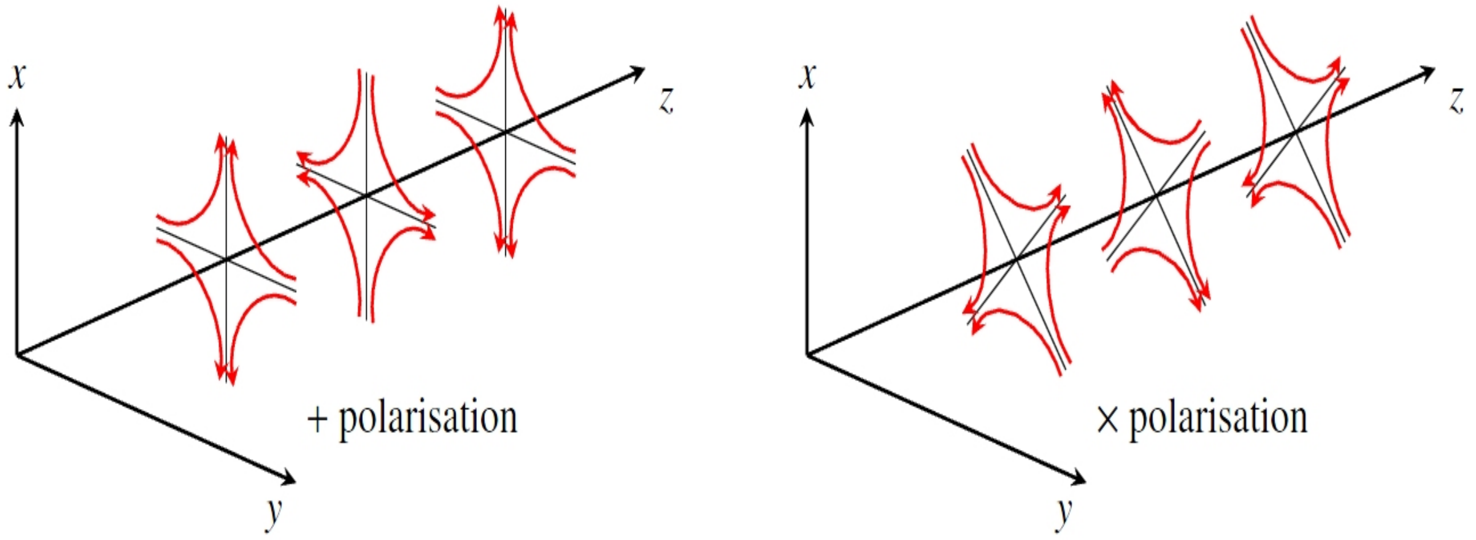

...but GWs *are* different...

- Coupling of GW to matter is very different from EM
- Very weak
  - $h \approx \delta L / L \approx 10^{-21} \dots 10^{-24}$
  - $h \approx 1 / r$
- Weakness
  - negligible scatter, absorption
  - perfect messengers!
- Huge energy flux
  - luminosity scale is $(c^5/G) \approx 3.6 \cdot 10^{59}$ erg/s

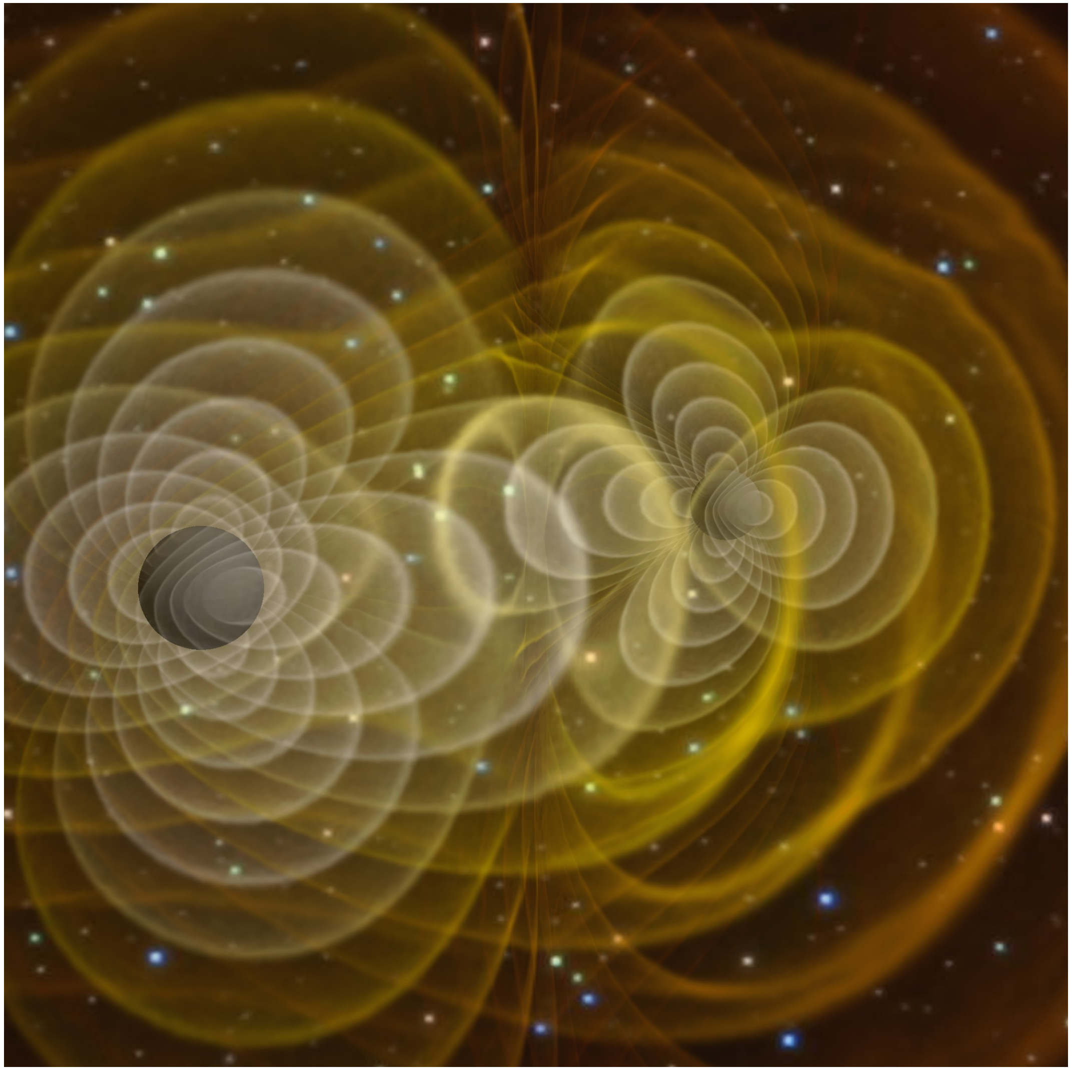

Evidence:
Hulse – Taylor Binary Pulsar discovered in 1974

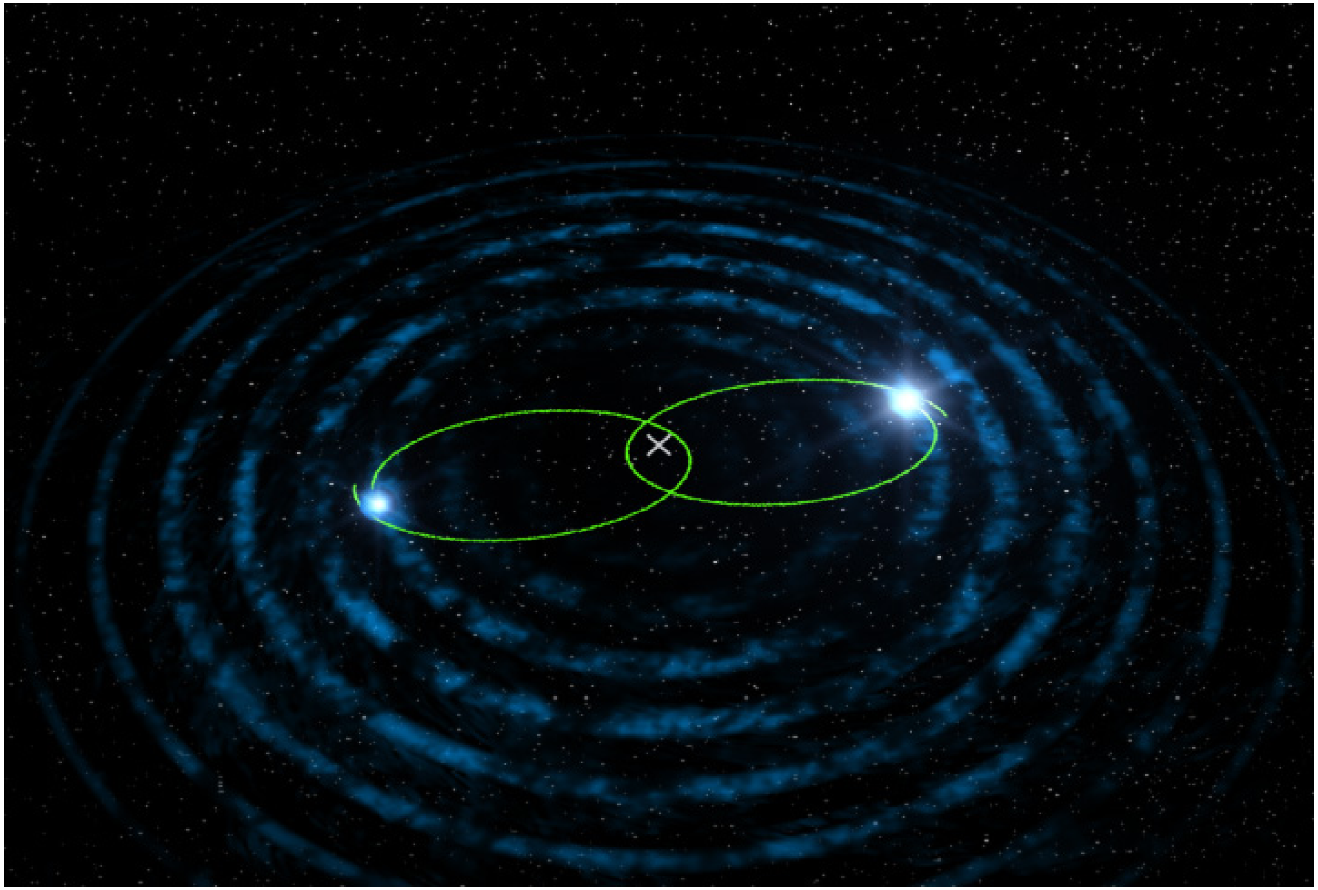

Evidence:
Hulse – Taylor Binary Pulsar discovered in 1974

- Orbital decay of PSR 1913 + 16 binary pulsar systems
  - from data points represent the cumulative shift of periastron time measured whereas the parabola curve shows the same quantity predicted by the General Relativity.
- Mass of both pulsars of about 1.4 solar masses.
- Orbital period: 7.75 hours.

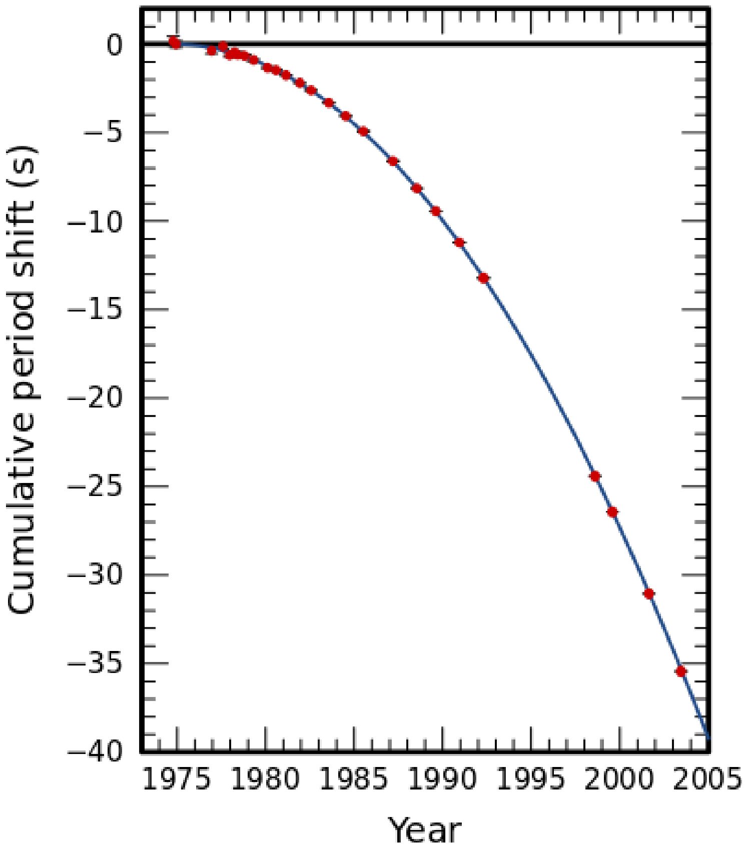

Existing Ground Based GW Detectors

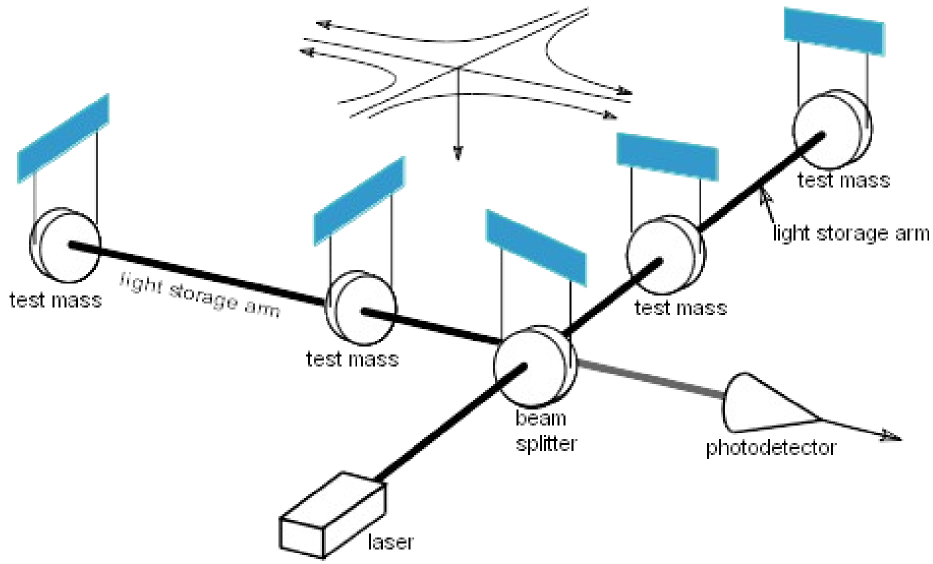

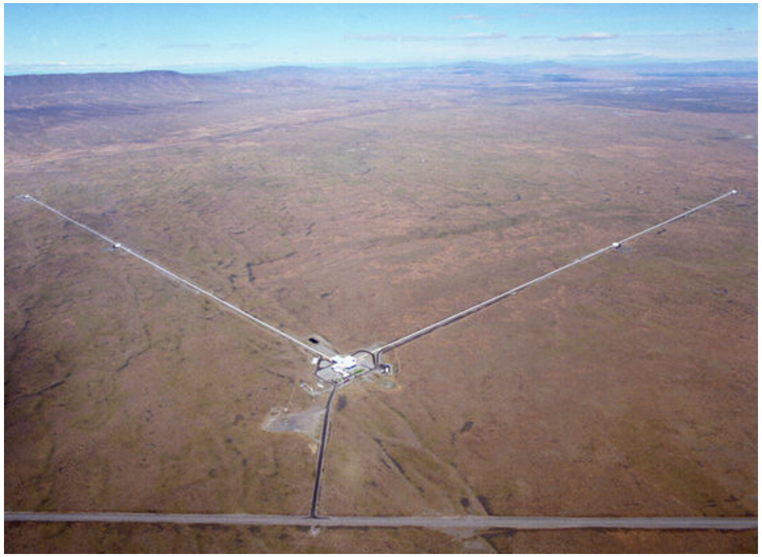

Existing/ Planned Ground Based GW Detectors

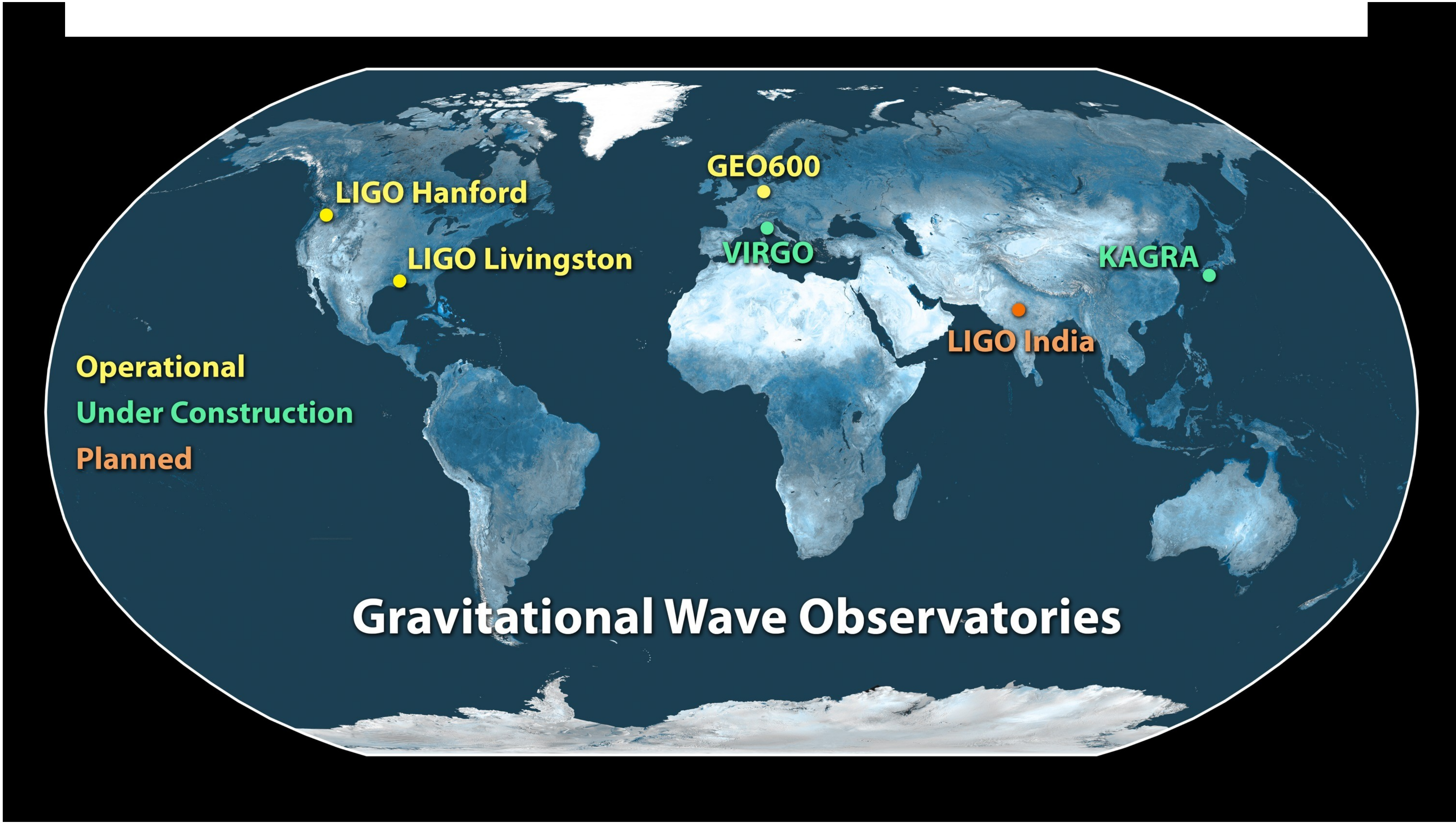

Gravitational wave signal of 14 September 2015

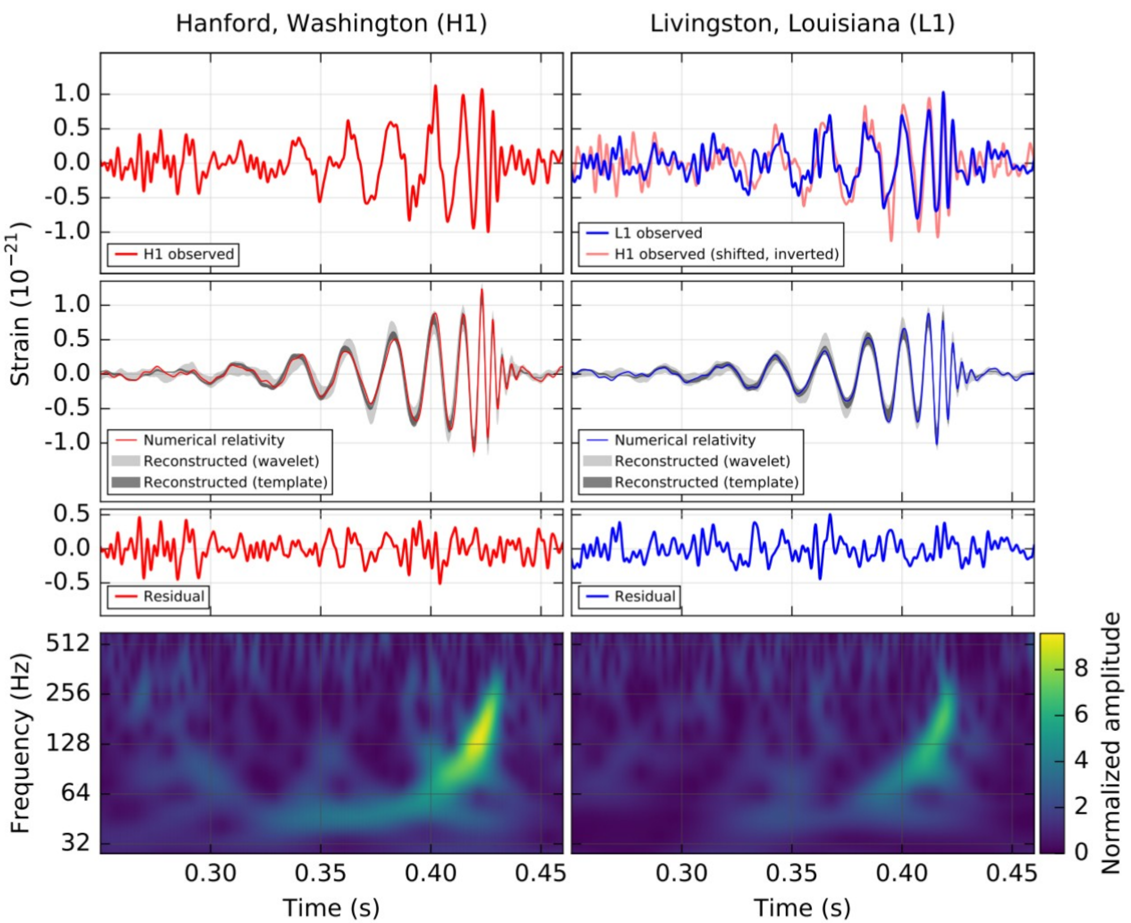

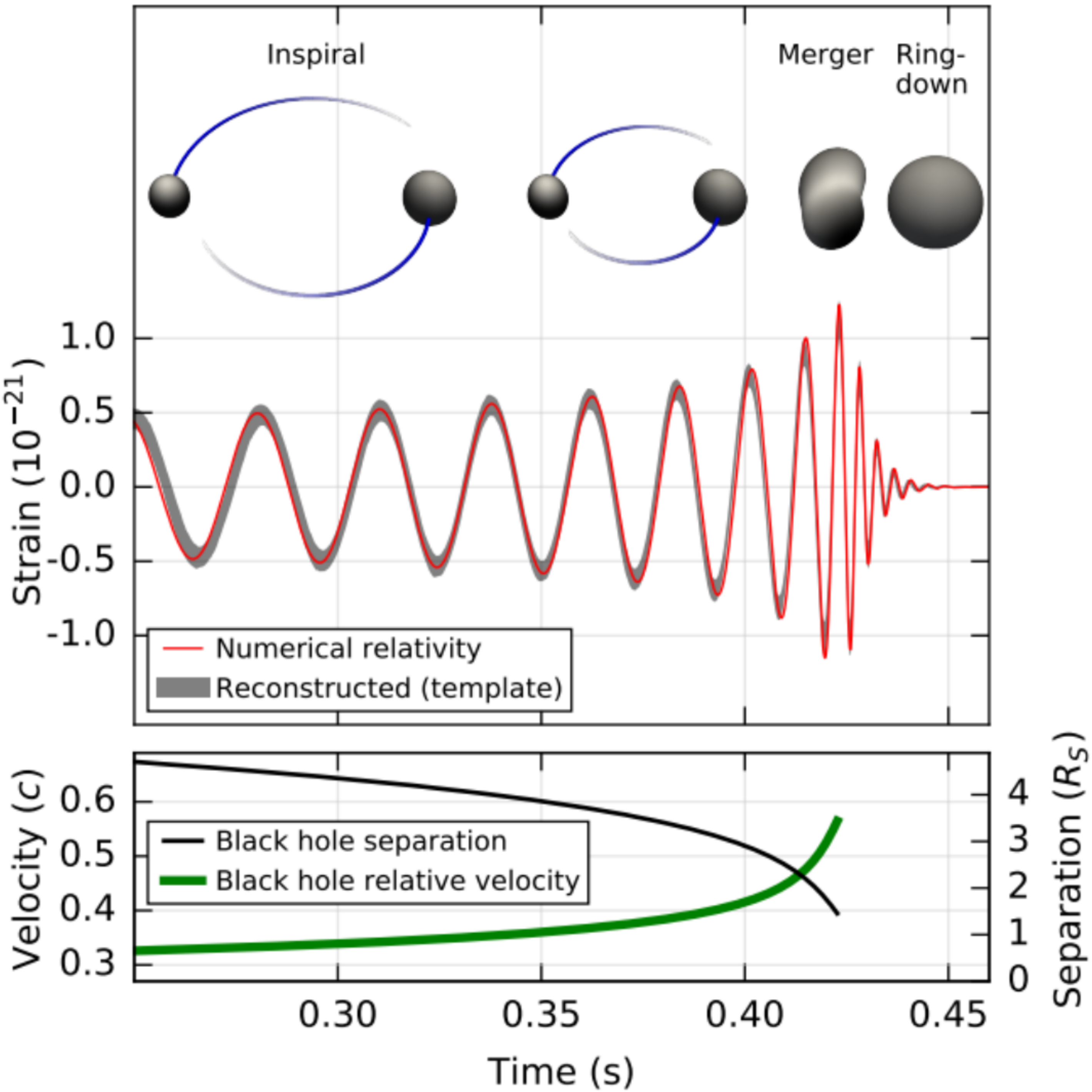

Inspiral
Merger
Ring-
down
Strain (10^{-21})
1.0
0.5
0.0
-0.5
-1.0
Numerical relativity
Reconstructed (template)
Velocity (c)
0.6
0.5
0.4
0.3
Black hole separation
Black hole relative velocity
Separation (R_S)
4
3
2
1
0
0.30
0.35
0.40
0.45
Time (s)

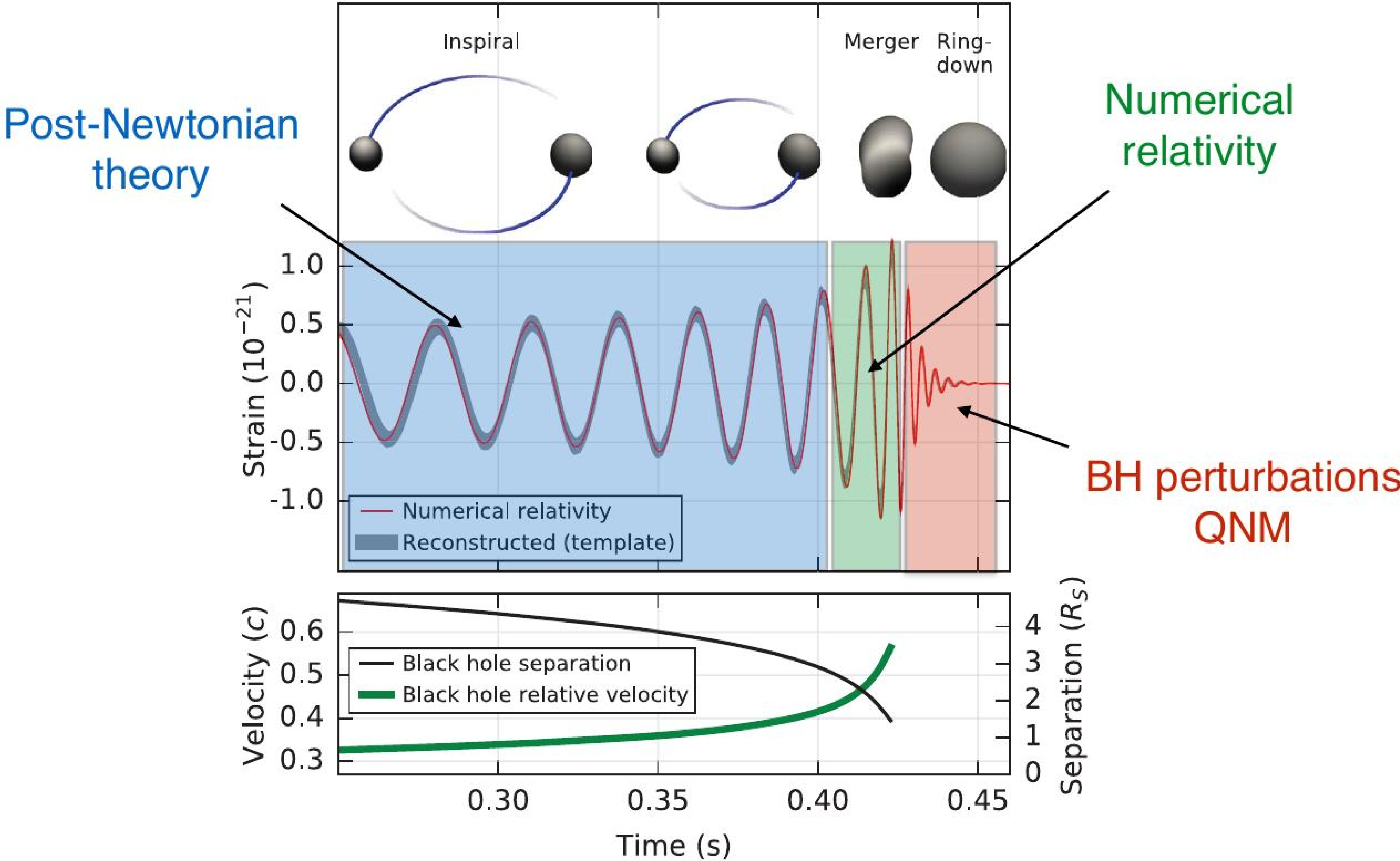

Post-Newtonian theory
Numerical relativity
BH perturbations QNM
Inspiral
Merger
Ring-down
Strain (10^{-21})
1.0
0.5
0.0
-0.5
-1.0
Numerical relativity
Reconstructed (template)
Velocity (c)
0.6
0.5
0.4
0.3
Black hole separation
Black hole relative velocity
Separation (R_S)
4
3
2
1
0
0.30
0.35
0.40
0.45
Time (s)

2-body Taylor-expanded N + 1PN + 2PN Hamiltonian

$$H_{\mathrm{N}}(\mathbf{x}_a, \mathbf{p}_a) = \frac{\mathbf{p}_1^2}{2m_1} - \frac{1}{2}\frac{Gm_1 m_2}{r_{12}} + (1 \leftrightarrow 2)$$

$$c^2 H_{1\mathrm{PN}}(\mathbf{x}_a, \mathbf{p}_a) = -\frac{1}{8}\frac{(\mathbf{p}_1^2)^2}{m_1^3} + \frac{1}{8}\frac{Gm_1 m_2}{r_{12}}\left(-12\frac{\mathbf{p}_1^2}{m_1^2} + 14\frac{(\mathbf{p}_1\cdot\mathbf{p}_2)}{m_1 m_2} + 2\frac{(\mathbf{n}_{12}\cdot\mathbf{p}_1)(\mathbf{n}_{12}\cdot\mathbf{p}_2)}{m_1 m_2}\right) + \frac{1}{4}\frac{Gm_1 m_2}{r_{12}}\frac{G(m_1+m_2)}{r_{12}} + (1 \leftrightarrow 2),$$

$$\begin{aligned} c^4 H_{2\mathrm{PN}}(\mathbf{x}_a, \mathbf{p}_a) = {} & \frac{1}{16}\frac{(\mathbf{p}_1^2)^3}{m_1^5} + \frac{1}{8}\frac{Gm_1 m_2}{r_{12}}\left(5\frac{(\mathbf{p}_1^2)^2}{m_1^4} - \frac{11}{2}\frac{\mathbf{p}_1^2\mathbf{p}_2^2}{m_1^2 m_2^2} - \frac{(\mathbf{p}_1\cdot\mathbf{p}_2)^2}{m_1^2 m_2^2} + 5\frac{\mathbf{p}_1^2(\mathbf{n}_{12}\cdot\mathbf{p}_2)^2}{m_1^2 m_2^2}\right. \\ & \left. - 6\frac{(\mathbf{p}_1\cdot\mathbf{p}_2)(\mathbf{n}_{12}\cdot\mathbf{p}_1)(\mathbf{n}_{12}\cdot\mathbf{p}_2)}{m_1^2 m_2^2} - \frac{3}{2}\frac{(\mathbf{n}_{12}\cdot\mathbf{p}_1)^2(\mathbf{n}_{12}\cdot\mathbf{p}_2)^2}{m_1^2 m_2^2}\right) \\ & + \frac{1}{4}\frac{G^2 m_1 m_2}{r_{12}^2}\left(m_2\left(10\frac{\mathbf{p}_1^2}{m_1^2} + 19\frac{\mathbf{p}_2^2}{m_2^2}\right) - \frac{1}{2}(m_1+m_2)\frac{27(\mathbf{p}_1\cdot\mathbf{p}_2) + 6(\mathbf{n}_{12}\cdot\mathbf{p}_1)(\mathbf{n}_{12}\cdot\mathbf{p}_2)}{m_1 m_2}\right) \\ & - \frac{1}{8}\frac{Gm_1 m_2}{r_{12}}\frac{G^2(m_1^2 + 5m_1 m_2 + m_2^2)}{r_{12}^2} + (1 \leftrightarrow 2), \end{aligned}$$

Post-Newtonian equations of motion (2-body, no spins)

2-body Taylor-expanded 3PN Hamiltonian [JS 98, DJS 01]

$$
\begin{aligned}
c^6 H_{3\mathrm{PN}}(\mathbf{x}_a,\mathbf{p}_a) = {} & -\frac{5}{128}\frac{(\mathbf{p}_1^2)^4}{m_1^7} + \frac{1}{32}\frac{G m_1 m_2}{r_{12}}\left(-14\frac{(\mathbf{p}_1^2)^3}{m_1^6} + 4\frac{((\mathbf{p}_1\cdot\mathbf{p}_2)^2 + 4\mathbf{p}_1^2\mathbf{p}_2^2)\mathbf{p}_1^2}{m_1^4 m_2^2} + 6\frac{\mathbf{p}_1^2(\mathbf{n}_{12}\cdot\mathbf{p}_1)^2(\mathbf{n}_{12}\cdot\mathbf{p}_2)^2}{m_1^4 m_2^2}\right.\\
& - 10\frac{(\mathbf{p}_1^2(\mathbf{n}_{12}\cdot\mathbf{p}_2)^2 + \mathbf{p}_2^2(\mathbf{n}_{12}\cdot\mathbf{p}_1)^2)\mathbf{p}_1^2}{m_1^4 m_2^2} + 24\frac{\mathbf{p}_1^2(\mathbf{p}_1\cdot\mathbf{p}_2)(\mathbf{n}_{12}\cdot\mathbf{p}_1)(\mathbf{n}_{12}\cdot\mathbf{p}_2)}{m_1^4 m_2^2}\\
& + 2\frac{\mathbf{p}_1^2(\mathbf{p}_1\cdot\mathbf{p}_2)(\mathbf{n}_{12}\cdot\mathbf{p}_2)^2}{m_1^3 m_2^3} + \frac{(7\mathbf{p}_1^2\mathbf{p}_2^2 - 10(\mathbf{p}_1\cdot\mathbf{p}_2)^2)(\mathbf{n}_{12}\cdot\mathbf{p}_1)(\mathbf{n}_{12}\cdot\mathbf{p}_2)}{m_1^3 m_2^3}\\
& + \frac{(\mathbf{p}_1^2\mathbf{p}_2^2 - 2(\mathbf{p}_1\cdot\mathbf{p}_2)^2)(\mathbf{p}_1\cdot\mathbf{p}_2)}{m_1^3 m_2^3} + 15\frac{(\mathbf{p}_1\cdot\mathbf{p}_2)(\mathbf{n}_{12}\cdot\mathbf{p}_1)^2(\mathbf{n}_{12}\cdot\mathbf{p}_2)^2}{m_1^3 m_2^3}\\
& \left. - 18\frac{\mathbf{p}_1^2(\mathbf{n}_{12}\cdot\mathbf{p}_1)(\mathbf{n}_{12}\cdot\mathbf{p}_2)^3}{m_1^3 m_2^3} + 5\frac{(\mathbf{n}_{12}\cdot\mathbf{p}_1)^3(\mathbf{n}_{12}\cdot\mathbf{p}_2)^3}{m_1^3 m_2^3}\right) + \frac{G^2 m_1 m_2}{r_{12}^2}\left(\frac{1}{16}(m_1 - 27 m_2)\frac{(\mathbf{p}_1^2)^2}{m_1^4}\right.\\
& - \frac{115}{16} m_1 \frac{\mathbf{p}_1^2(\mathbf{p}_1\cdot\mathbf{p}_2)}{m_1^3 m_2} + \frac{1}{48} m_2 \frac{25(\mathbf{p}_1\cdot\mathbf{p}_2)^2 + 371\mathbf{p}_1^2\mathbf{p}_2^2}{m_1^2 m_2^2} + \frac{17}{16}\frac{\mathbf{p}_1^2(\mathbf{n}_{12}\cdot\mathbf{p}_1)^2}{m_1^3} + \frac{5}{12}\frac{(\mathbf{n}_{12}\cdot\mathbf{p}_1)^4}{m_1^3}\\
& - \frac{1}{8} m_1 \frac{(15\mathbf{p}_1^2(\mathbf{n}_{12}\cdot\mathbf{p}_2) + 11(\mathbf{p}_1\cdot\mathbf{p}_2)(\mathbf{n}_{12}\cdot\mathbf{p}_1))(\mathbf{n}_{12}\cdot\mathbf{p}_1)}{m_1^3 m_2} - \frac{3}{2} m_1 \frac{(\mathbf{n}_{12}\cdot\mathbf{p}_1)^3(\mathbf{n}_{12}\cdot\mathbf{p}_2)}{m_1^3 m_2}\\
& + \frac{125}{12} m_2 \frac{(\mathbf{p}_1\cdot\mathbf{p}_2)(\mathbf{n}_{12}\cdot\mathbf{p}_1)(\mathbf{n}_{12}\cdot\mathbf{p}_2)}{m_1^2 m_2^2} + \frac{10}{3} m_2 \frac{(\mathbf{n}_{12}\cdot\mathbf{p}_1)^2(\mathbf{n}_{12}\cdot\mathbf{p}_2)^2}{m_1^2 m_2^2}\\
& \left. - \frac{1}{48}(220 m_1 + 193 m_2)\frac{\mathbf{p}_1^2(\mathbf{n}_{12}\cdot\mathbf{p}_2)^2}{m_1^2 m_2^2}\right) + \frac{G^3 m_1 m_2}{r_{12}^3}\left(-\frac{1}{48}\left(425 m_1^2 + \left(473 - \frac{3}{4}\pi^2\right) m_1 m_2 + 150 m_2^2\right)\frac{\mathbf{p}_1^2}{m_1^2}\right.\\
& + \frac{1}{16}\left(77(m_1^2 + m_2^2) + \left(143 - \frac{1}{4}\pi^2\right) m_1 m_2\right)\frac{(\mathbf{p}_1\cdot\mathbf{p}_2)}{m_1 m_2} + \frac{1}{16}\left(20 m_1^2 - \left(43 + \frac{3}{4}\pi^2\right) m_1 m_2\right)\frac{(\mathbf{n}_{12}\cdot\mathbf{p}_1)^2}{m_1^2}\\
& \left. + \frac{1}{16}\left(21(m_1^2 + m_2^2) + \left(119 + \frac{3}{4}\pi^2\right) m_1 m_2\right)\frac{(\mathbf{n}_{12}\cdot\mathbf{p}_1)(\mathbf{n}_{12}\cdot\mathbf{p}_2)}{m_1 m_2}\right)\\
& + \frac{1}{8}\frac{G^4 m_1 m_2^3}{r_{12}^4}\left(\left(\frac{227}{3} - \frac{21}{4}\pi^2\right) m_1 + m_2\right) + (1 \leftrightarrow 2).
\end{aligned}
$$

See papers by Damour, Jaranowski and Schaefer (now known up to 4PN)

Taylor-expanded 3.5PN waveform

Blanchet,Iyer, Joguet 02, Blanchet, Damour, Esposito-Farese, Iyer 04, Kidder 07, Blanchet et al. 08, Faye et al '12, Bohé, Marsat, Blanchet, Buonanno 13-15

$$h^{22} = -8\sqrt{\frac{\pi}{5}}\frac{G\nu m}{c^2 R}e^{-2i\phi}x\Big\{1 - x\Big(\frac{107}{42} - \frac{55}{42}\nu\Big) + x^{3/2}\Big[2\pi + 6i\ln\Big(\frac{x}{x_0}\Big)\Big] - x^2\Big(\frac{2173}{1512} + \frac{1069}{216}\nu - \frac{2047}{1512}\nu^2\Big)$$
$$- x^{5/2}\Big[\Big(\frac{107}{21} - \frac{34}{21}\nu\Big)\pi + 24i\nu + \Big(\frac{107i}{7} - \frac{34i}{7}\nu\Big)\ln\Big(\frac{x}{x_0}\Big)\Big]$$
$$+ x^3\Big[\frac{27\,027\,409}{646\,800} - \frac{856}{105}\gamma_E + \frac{2}{3}\pi^2 - \frac{1712}{105}\ln 2 - \frac{428}{105}\ln x$$
$$- 18\Big[\ln\Big(\frac{x}{x_0}\Big)\Big]^2 - \Big(\frac{278\,185}{33\,264} - \frac{41}{96}\pi^2\Big)\nu - \frac{20\,261}{2772}\nu^2 + \frac{114\,635}{99\,792}\nu^3 + \frac{428i}{105}\pi + 12i\pi\ln\Big(\frac{x}{x_0}\Big)\Big] + O(\epsilon^{7/2})\Big\},$$

$$x = (M\Omega)^{2/3} \sim v^2/c^2$$

$$M = m_1 + m_2$$
$$\nu = m_1 m_2/(m_1 + m_2)^2$$

Waveform for the gravitational radiation (to lowest order is just the quadrupole formula derived by Einstein)

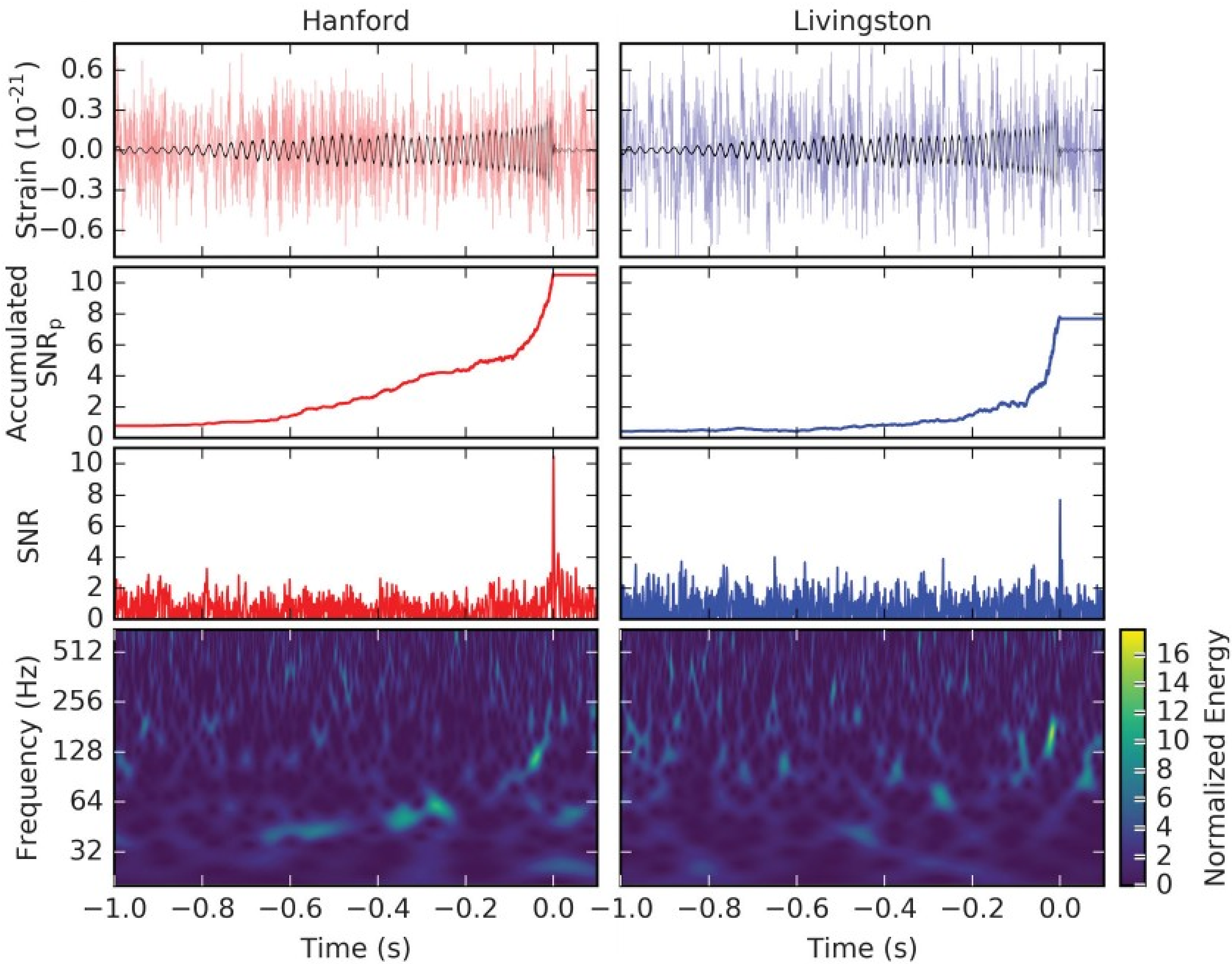

GW151226 observed by the LIGO Hanford (left column) and Livingston (right column) detectors, where times are relative to December 26, 2015 at 03:38:53.648 UTC.

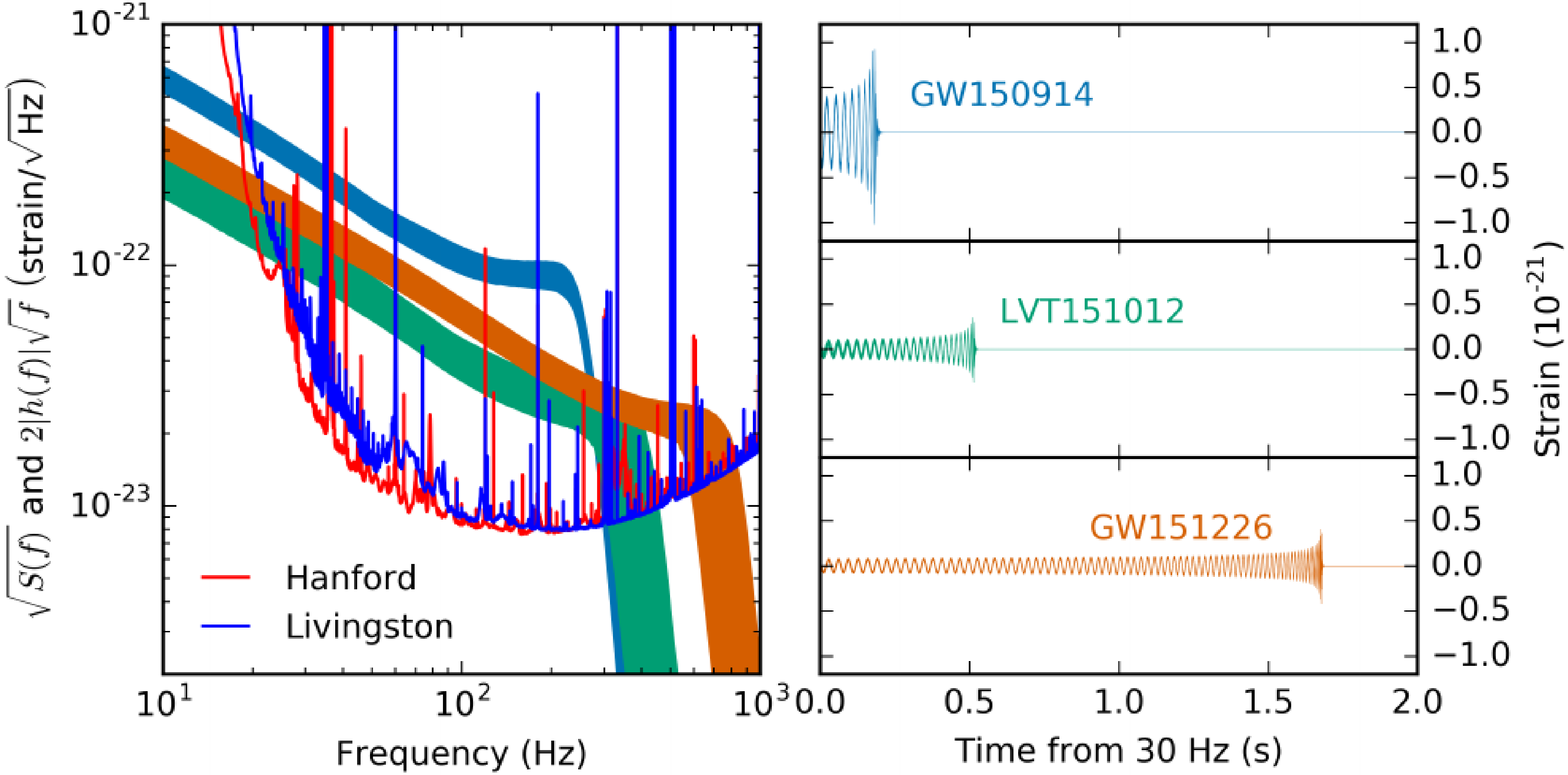

FIG. 1. Left: Amplitude spectral density of the total strain noise of the H1 and L1 detectors, $\sqrt{S(f)}$, in units of strain per $\sqrt{\text{Hz}}$, and the recovered signals of GW150914, GW151226 and LVT151012 plotted so that the relative amplitudes can be related to the SNR of the signal (as described in the text). Right: Time evolution of the waveforms from when they enter the detectors' sensitive band at 30 Hz. All bands show the 90% credible regions of the LIGO Hanford signal reconstructions from a coherent Bayesian analysis using a non-precessing spin waveform model [45].

Event	GW150914	GW151226	LVT151012
Signal-to-noise ratio ρ	23.7	13.0	9.7
False alarm rate $\mathrm{FAR}/\mathrm{yr}^{-1}$	$< 6.0 \times 10^{-7}$	$< 6.0 \times 10^{-7}$	0.37
p-value	7.5×10^{-8}	7.5×10^{-8}	0.045
Significance	$> 5.3\,\sigma$	$> 5.3\,\sigma$	1.7σ
Primary mass $m_1^{\mathrm{source}}/\mathrm{M}_\odot$	$36.2^{+5.2}_{-3.8}$	$14.2^{+8.3}_{-3.7}$	23^{+18}_{-6}
Secondary mass $m_2^{\mathrm{source}}/\mathrm{M}_\odot$	$29.1^{+3.7}_{-4.4}$	$7.5^{+2.3}_{-2.3}$	13^{+4}_{-5}
Chirp mass $\mathscr{M}^{\mathrm{source}}/\mathrm{M}_\odot$	$28.1^{+1.8}_{-1.5}$	$8.9^{+0.3}_{-0.3}$	$15.1^{+1.4}_{-1.1}$
Total mass $M^{\mathrm{source}}/\mathrm{M}_\odot$	$65.3^{+4.1}_{-3.4}$	$21.8^{+5.9}_{-1.7}$	37^{+13}_{-4}
Effective inspiral spin χ_{eff}	$-0.06^{+0.14}_{-0.14}$	$0.21^{+0.20}_{-0.10}$	$0.0^{+0.3}_{-0.2}$
Final mass $M_f^{\mathrm{source}}/\mathrm{M}_\odot$	$62.3^{+3.7}_{-3.1}$	$20.8^{+6.1}_{-1.7}$	35^{+14}_{-4}
Final spin a_f	$0.68^{+0.05}_{-0.06}$	$0.74^{+0.06}_{-0.06}$	$0.66^{+0.09}_{-0.10}$
Radiated energy $E_{\mathrm{rad}}/(\mathrm{M}_\odot c^2)$	$3.0^{+0.5}_{-0.4}$	$1.0^{+0.1}_{-0.2}$	$1.5^{+0.3}_{-0.4}$
Peak luminosity $\ell_{\mathrm{peak}}/(\mathrm{erg\,s^{-1}})$	$3.6^{+0.5}_{-0.4} \times 10^{56}$	$3.3^{+0.8}_{-1.6} \times 10^{56}$	$3.1^{+0.8}_{-1.8} \times 10^{56}$
Luminosity distance D_L/Mpc	420^{+150}_{-180}	440^{+180}_{-190}	1000^{+500}_{-500}
Source redshift z	$0.09^{+0.03}_{-0.04}$	$0.09^{+0.03}_{-0.04}$	$0.20^{+0.09}_{-0.09}$
Sky localization $\Delta\Omega/\mathrm{deg}^2$	230	850	1600

4 January 2017: third event 50-Solar-Mass Binary Black Hole Coalescence at Redshift 0.2

Coalescence of
a 31.2 and a 19.4
Solar mass BH,
giving rise to a 48.7
Solar mass
Black Hole.

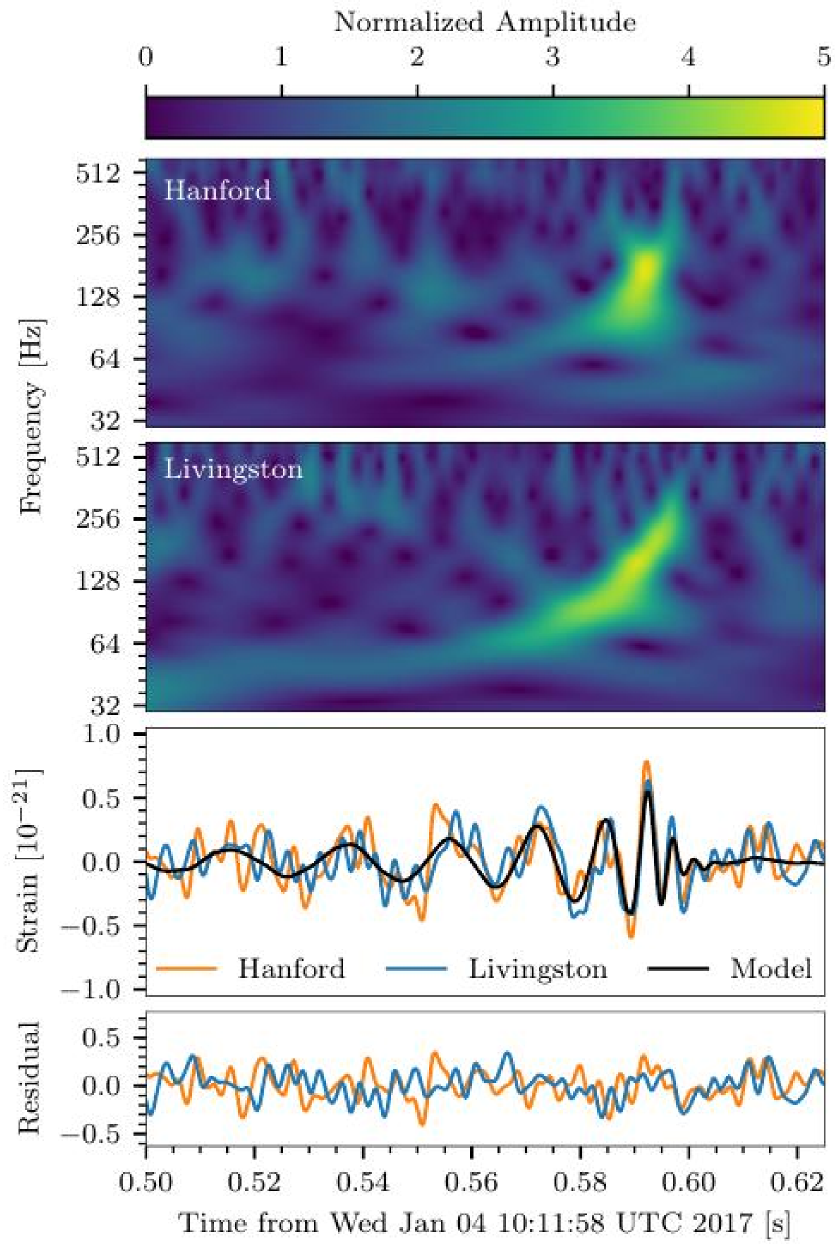

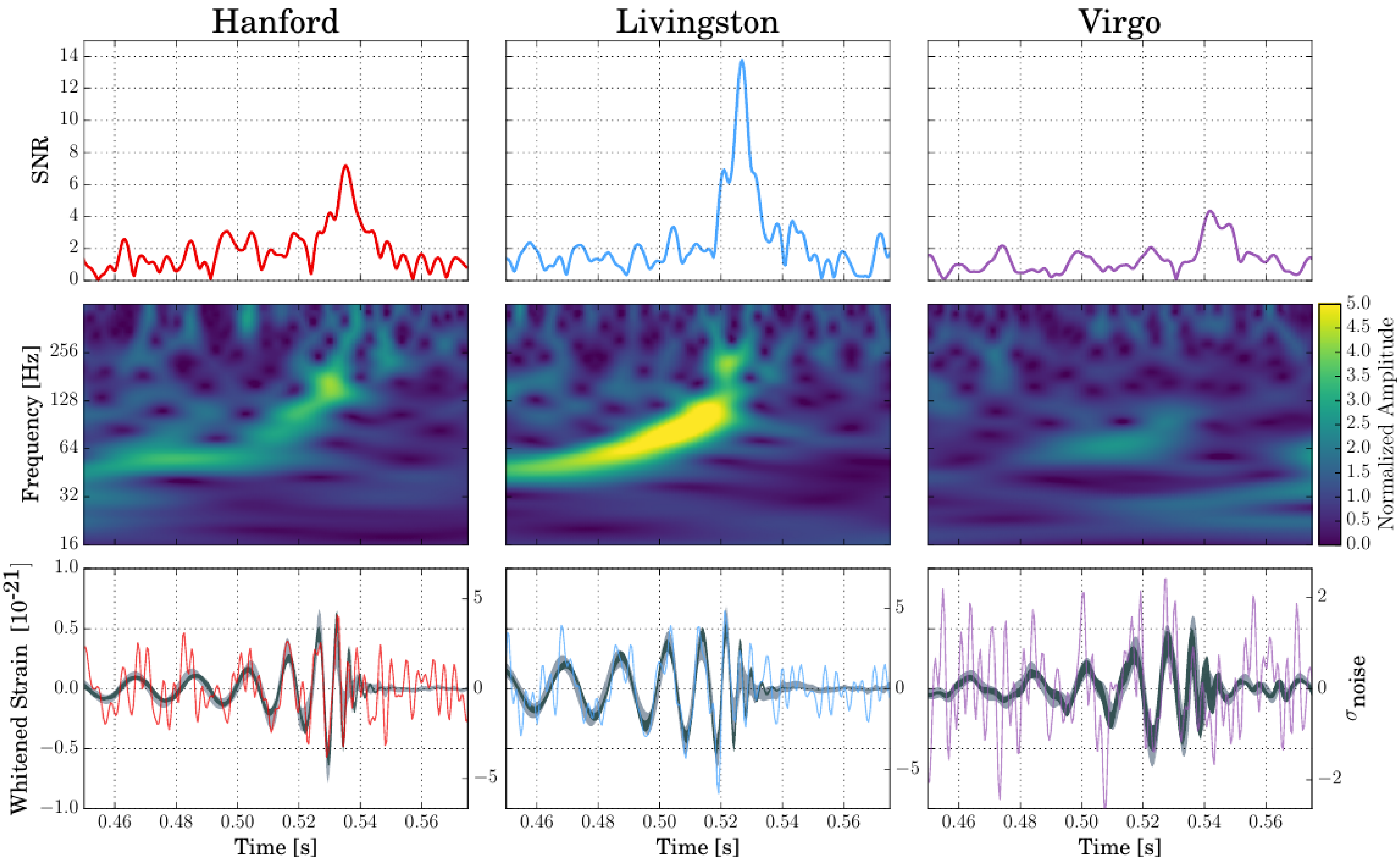

Ereigniss vom 14 August 2017: 30 + 25 Sonnemassen; Endmasse 53

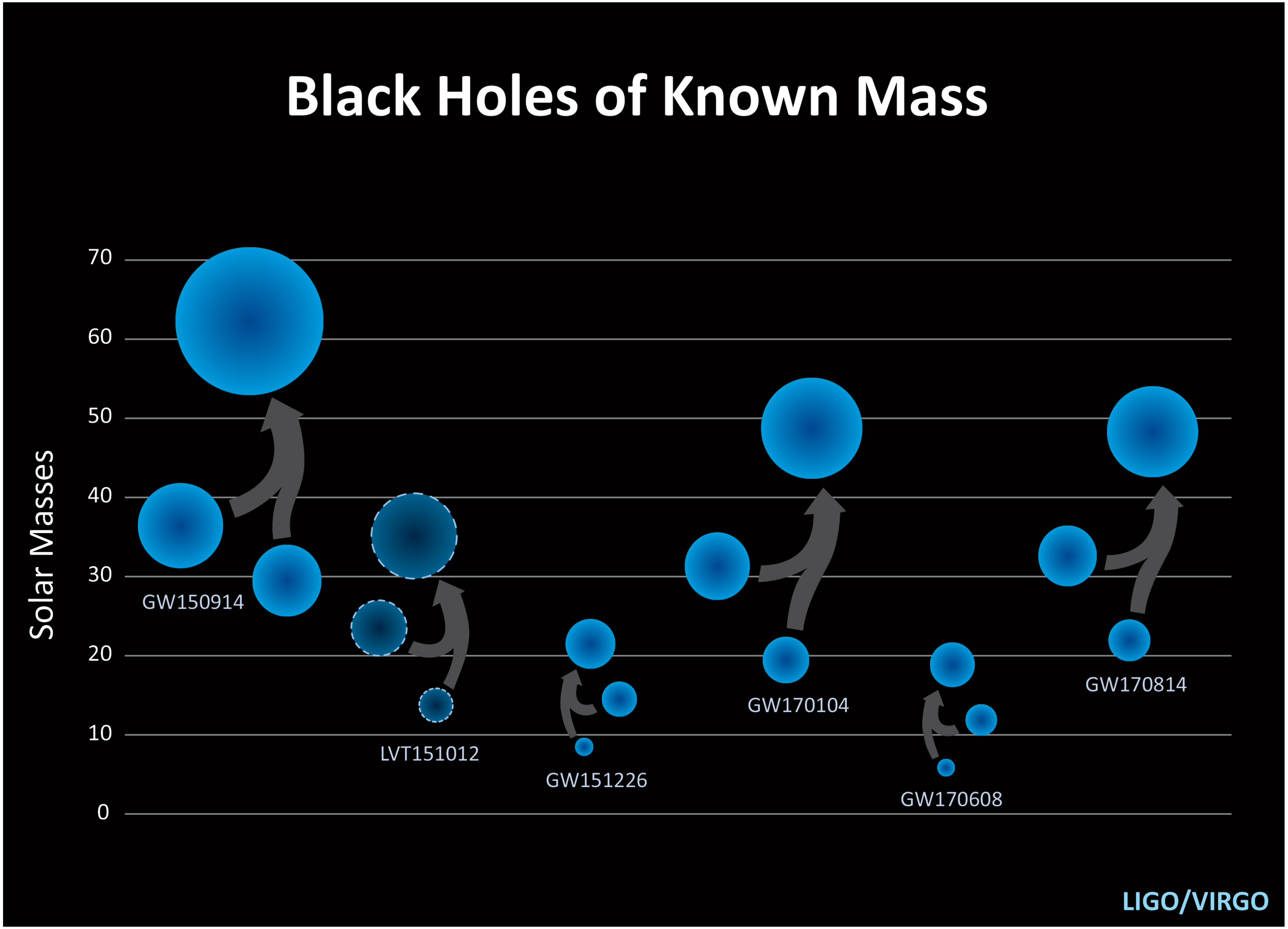

Black holes discovered so far by gravitational wave observations

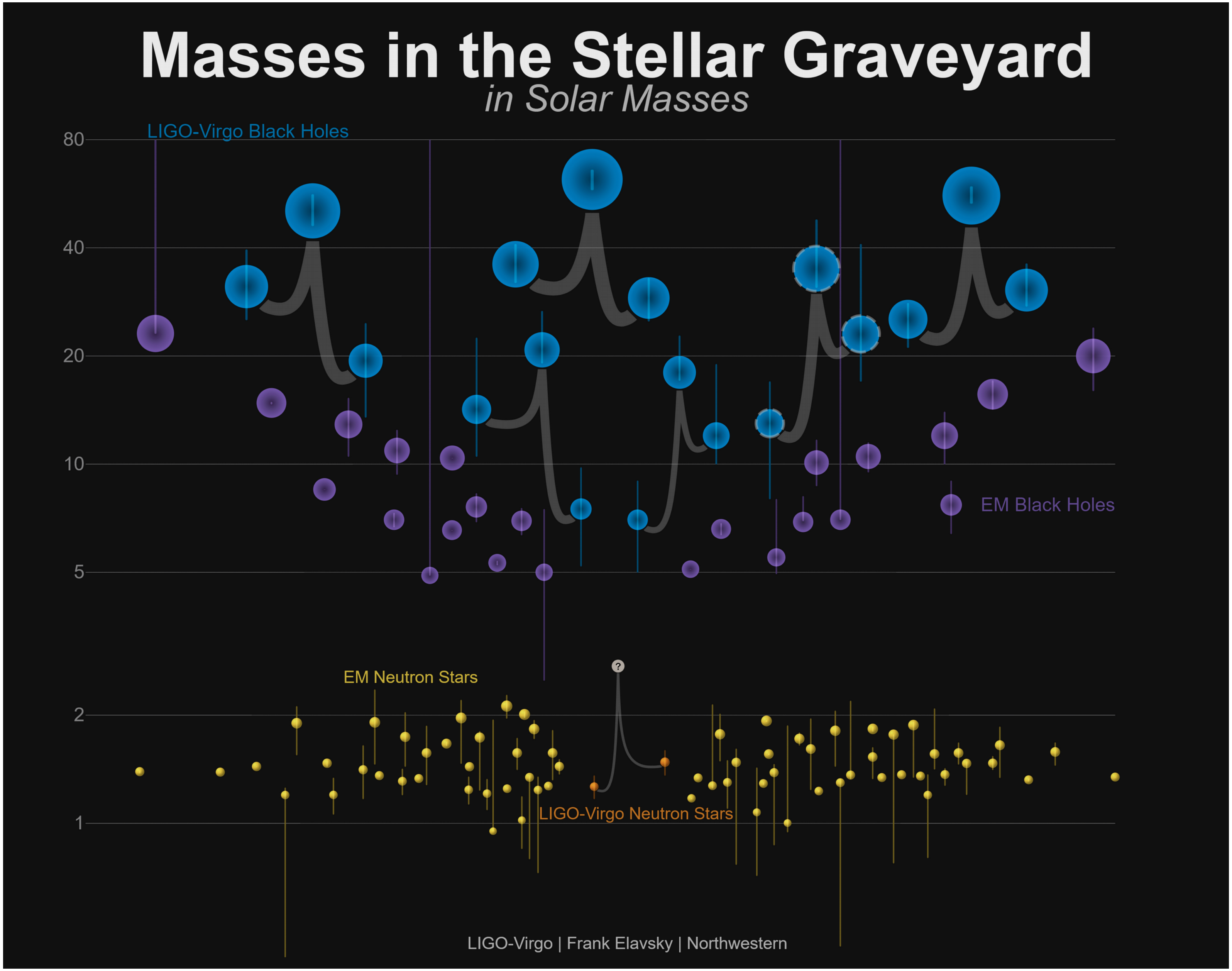

Blue/Orange: black holes/neutron stars discovered by GW
Purple: black holes discovered via electromagnetic observations
Yellow: neutron stars with electromagnetic observations

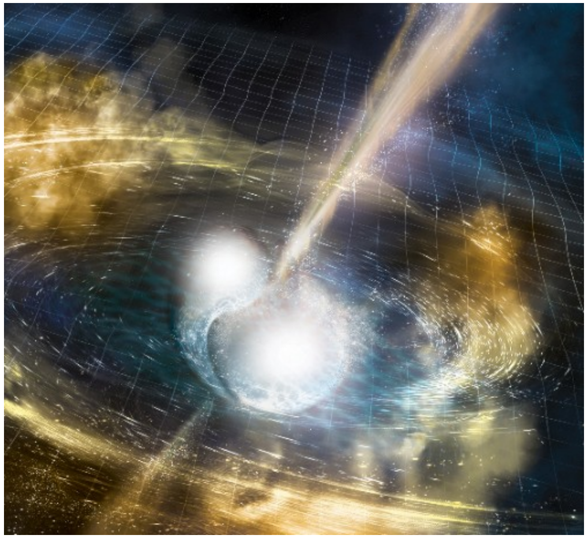

Artist's illustration of two merging Neutron stars.

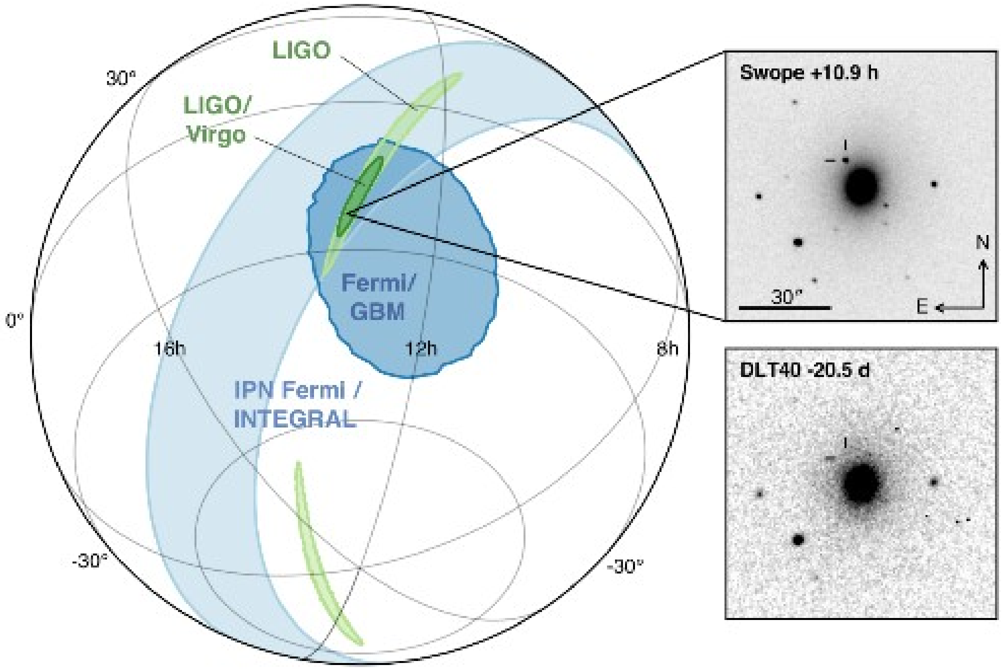

Discovery of the optical image by the Swope Telescope.
Host galaxy NGC 4993.
Top: 10.9 hr after the merger.
Bottom: 20.5 days before.

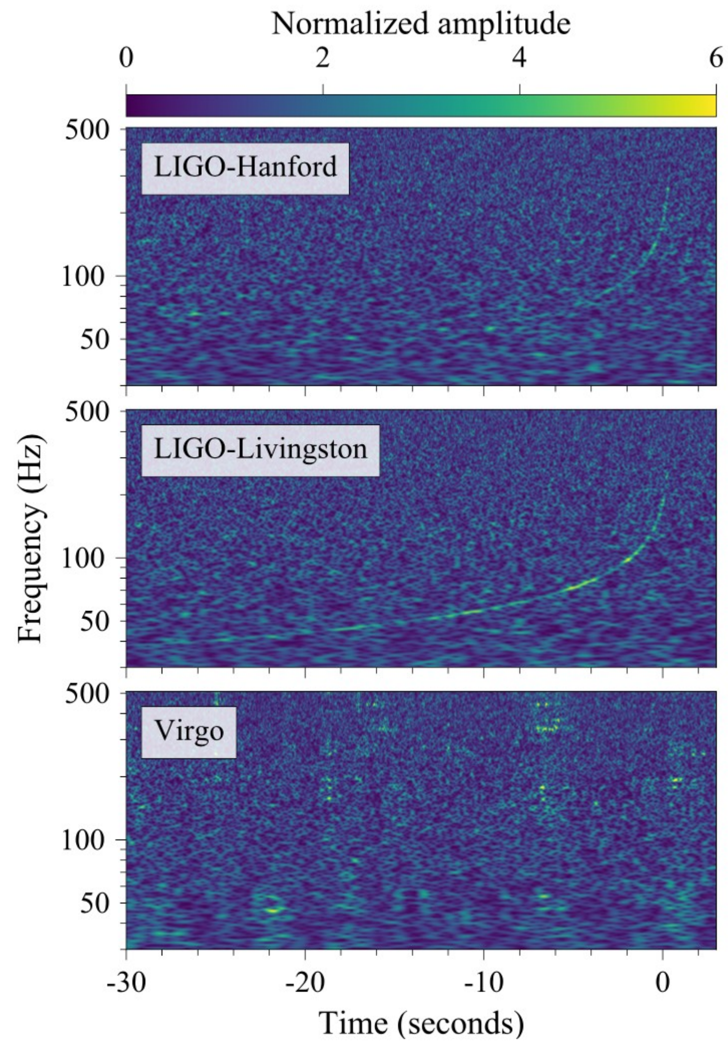

Time-frequency representations of data containing the gravitational-wave event GW170817 by LIGO and VIRGO.

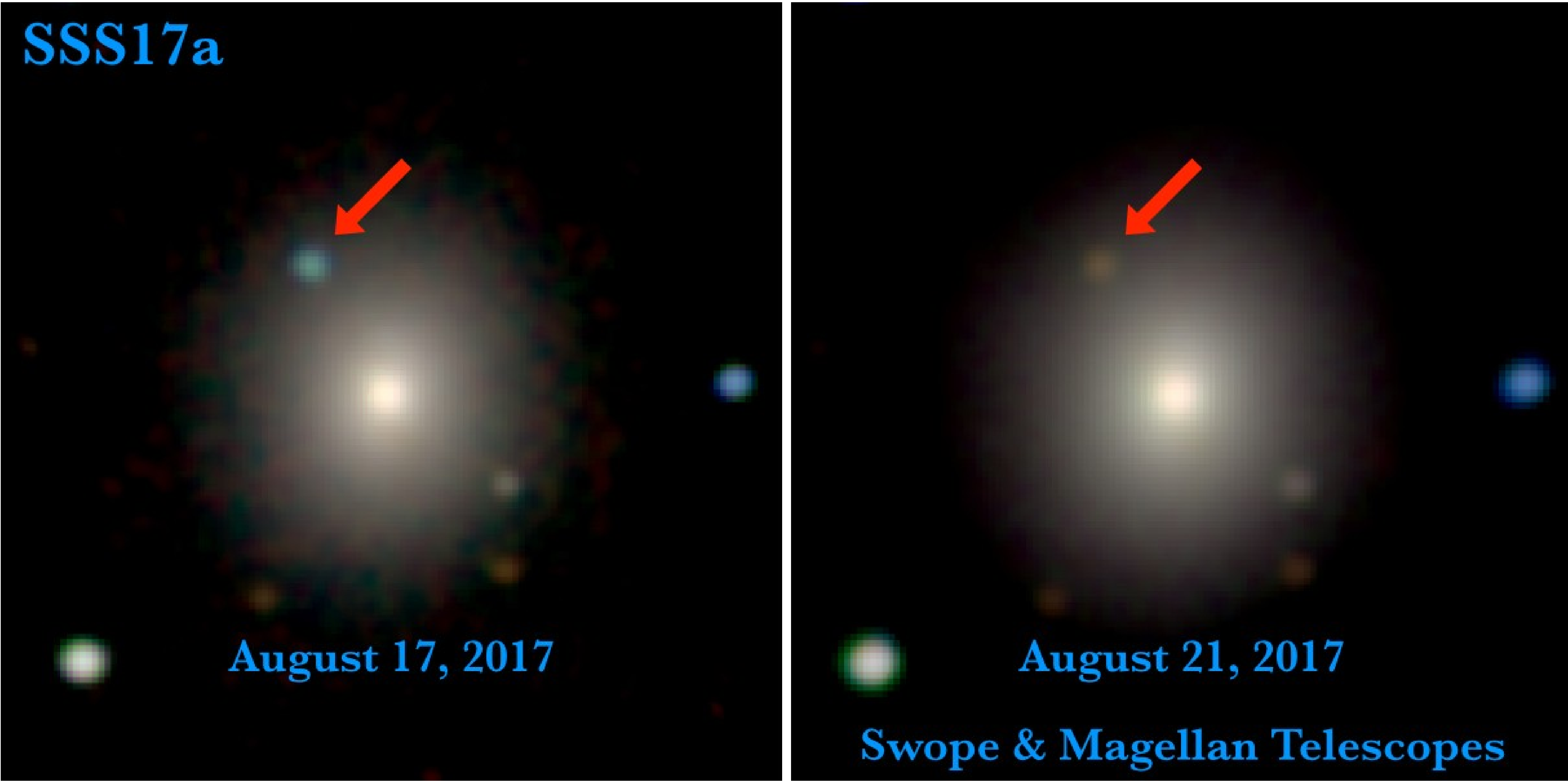

The left image was taken just 11 hours after the GW detection.

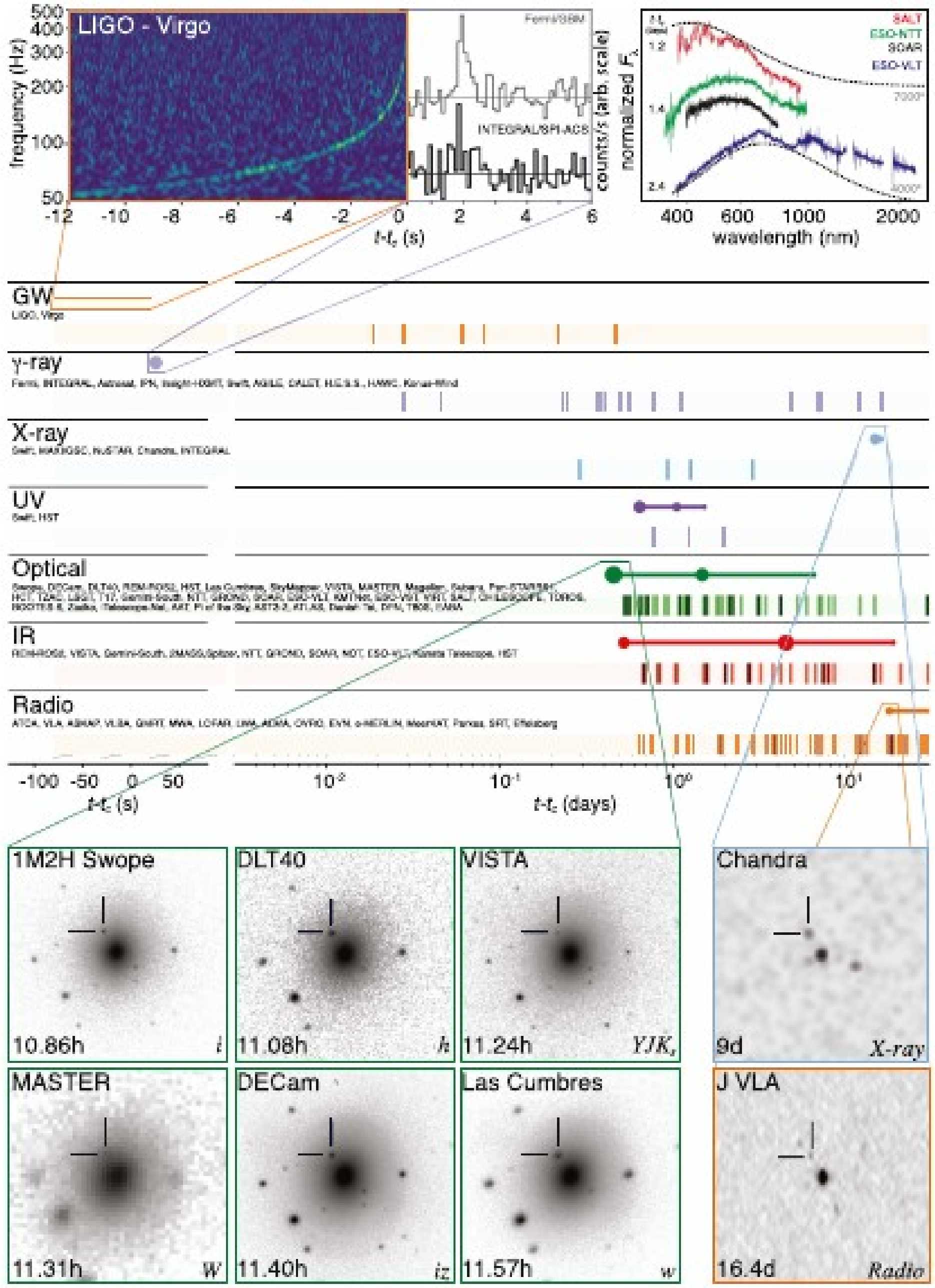

Time line of the discovery of GW170817 in the various electromagnetic bands.

GW170817

Binary neutron star merger

A LIGO / Virgo gravitational wave detection with associated electromagnetic events observed by over 70 observatories.

Distance
130 million light years

Discovered
17 August 2017

Type
Neutron star merger

12:41:04 UTC
A gravitational wave from a binary neutron star merger is detected.

gravitational wave signal
Two neutron stars, each the size of a city but with at least the mass of the sun, collided with each other.

gamma ray burst
A short gamma ray burst is an intense beam of gamma ray radiation which is produced just after the merger.

+ 2 seconds
A gamma ray burst is detected.

+10 hours 52 minutes
A new bright source of optical light is detected in a galaxy called NGC 4993, in the constellation of Hydra.

kilonova
Decaying neutron-rich material creates a glowing kilonova, producing heavy metals like gold and platinum.

+11 hours 36 minutes
Infrared emission observed.

+15 hours
Bright ultraviolet emission detected.

+9 days
X-ray emission detected.

radio remnant
As material moves away from the merger it produces a shockwave in the interstellar medium - the tenuous material between stars. This produces emission which can last for years.

+16 days
Radio emission detected.

GW170817 allows us to measure the expansion rate of the universe directly using gravitational waves for the first time.

Detecting gravitational waves from a neutron star merger allows us to find out more about the structure of these unusual objects.

This multimessenger event provides confirmation that neutron star mergers can produce short gamma ray bursts.

Au

The observation of a kilonova allowed us to show that neutron star mergers could be responsible for the production of most of the heavy elements, like gold, in the universe.

Observing both electromagnetic and gravitational waves from the event provides compelling evidence that gravitational waves travel at the same speed as light.

Different Sources – Different Signals

Binary White Dwarfs,
Neutron Stars,
Stellar Black Holes

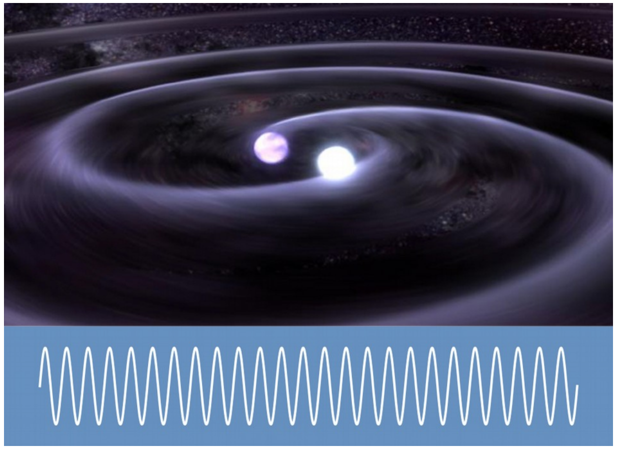

Extreme
Mass-Ratio
In-Spirals (EMRI)

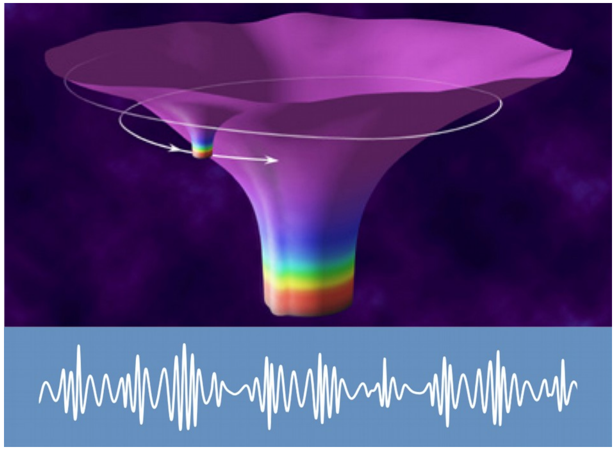

Different Sources – Different Signals

Coalescence of Supermassive Black Holes

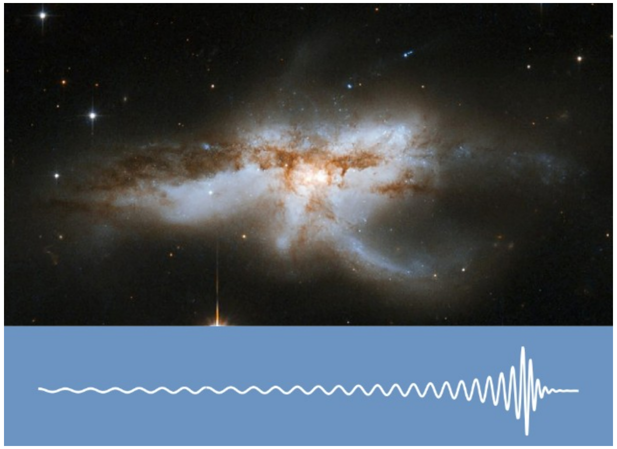

Primordial Gravitational Waves

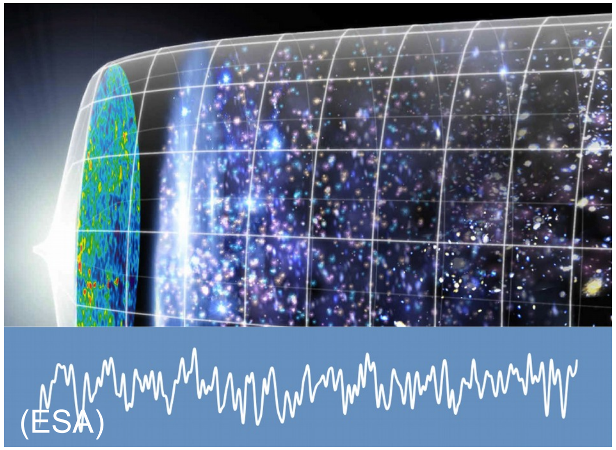

The Gravitational Wave Spectrum

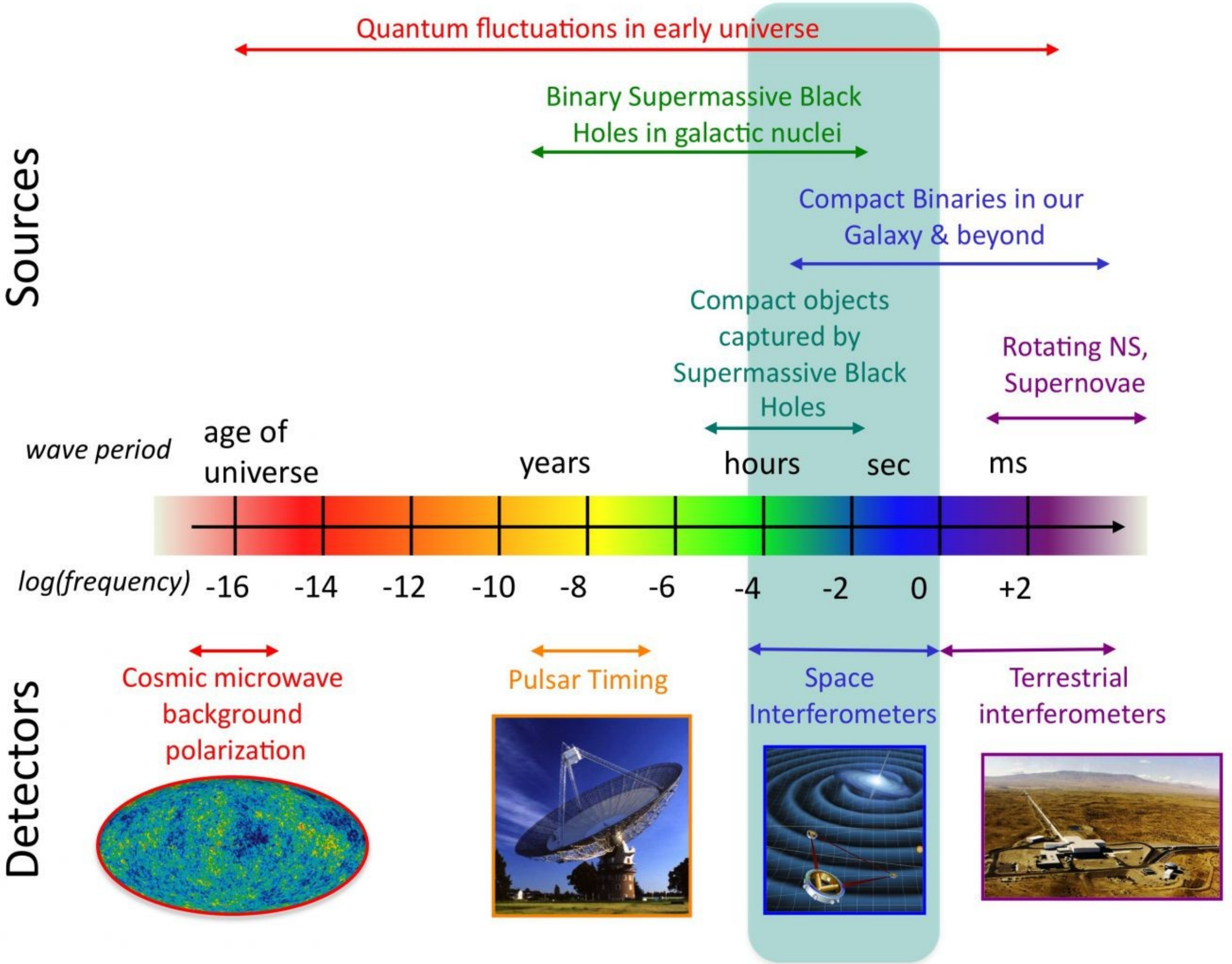

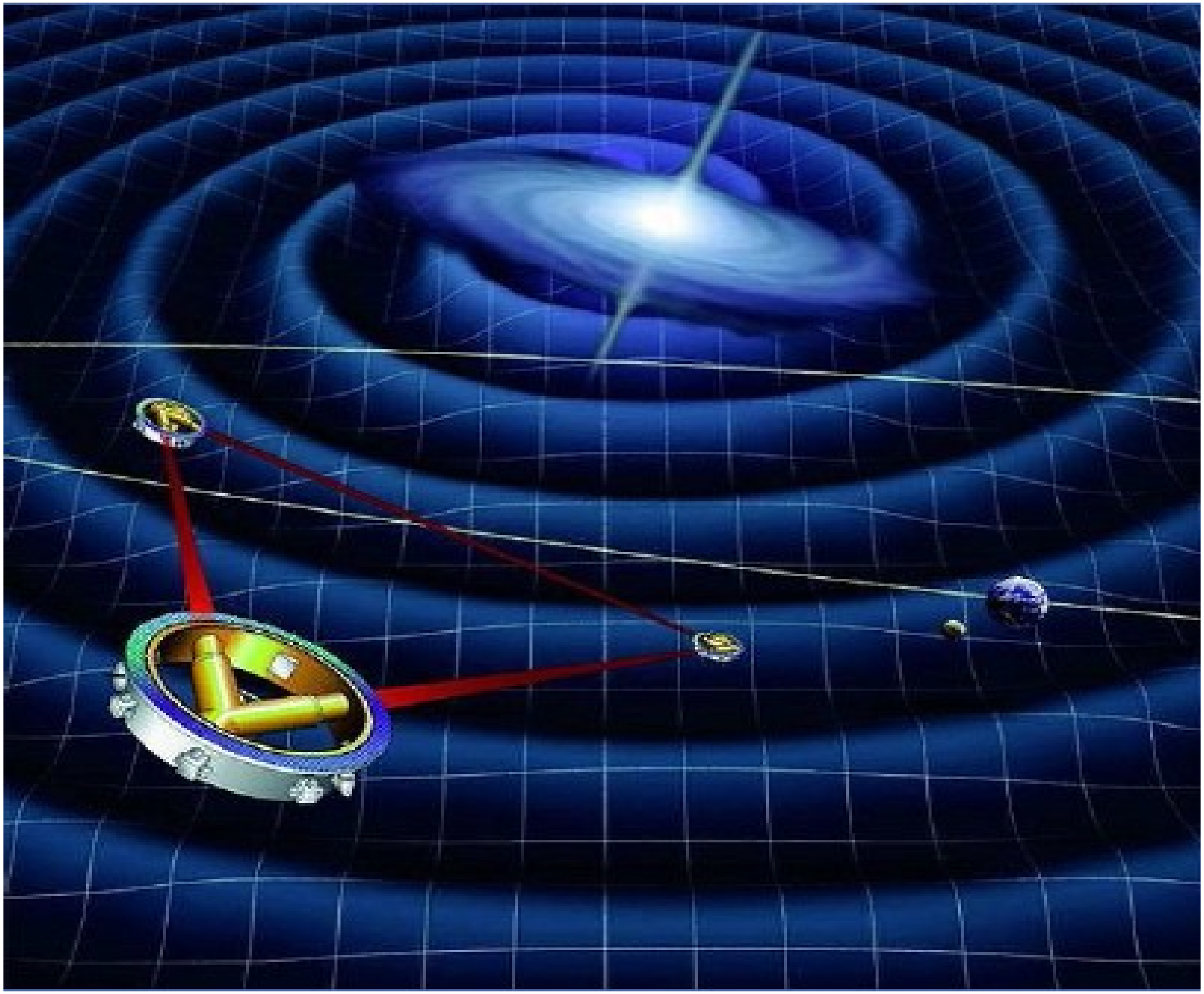

LISA (Laser Interferometer Space Antenna)

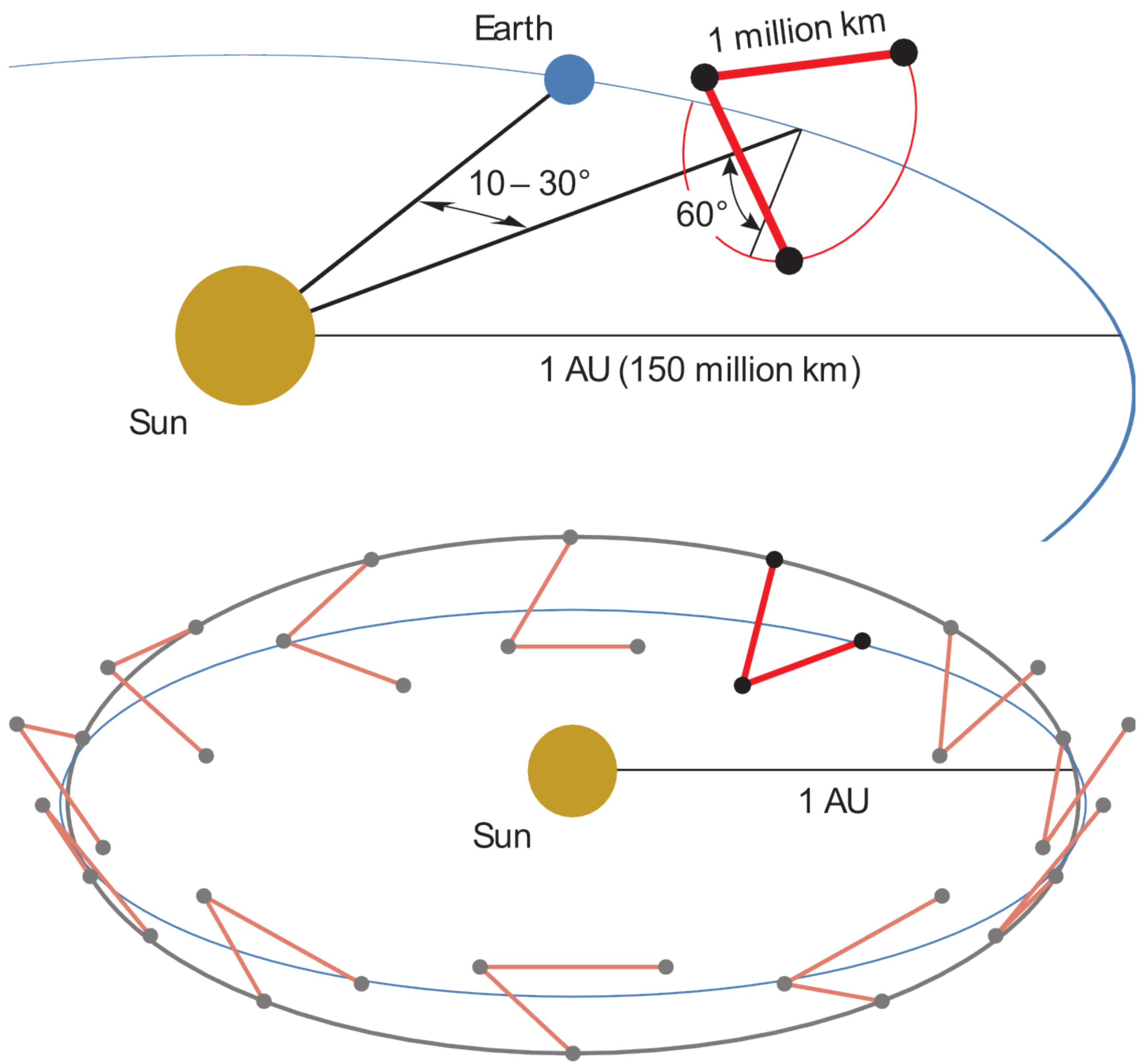

Earth
1 million km
10 – 30°
60°
1 AU (150 million km)
Sun
Sun
1 AU

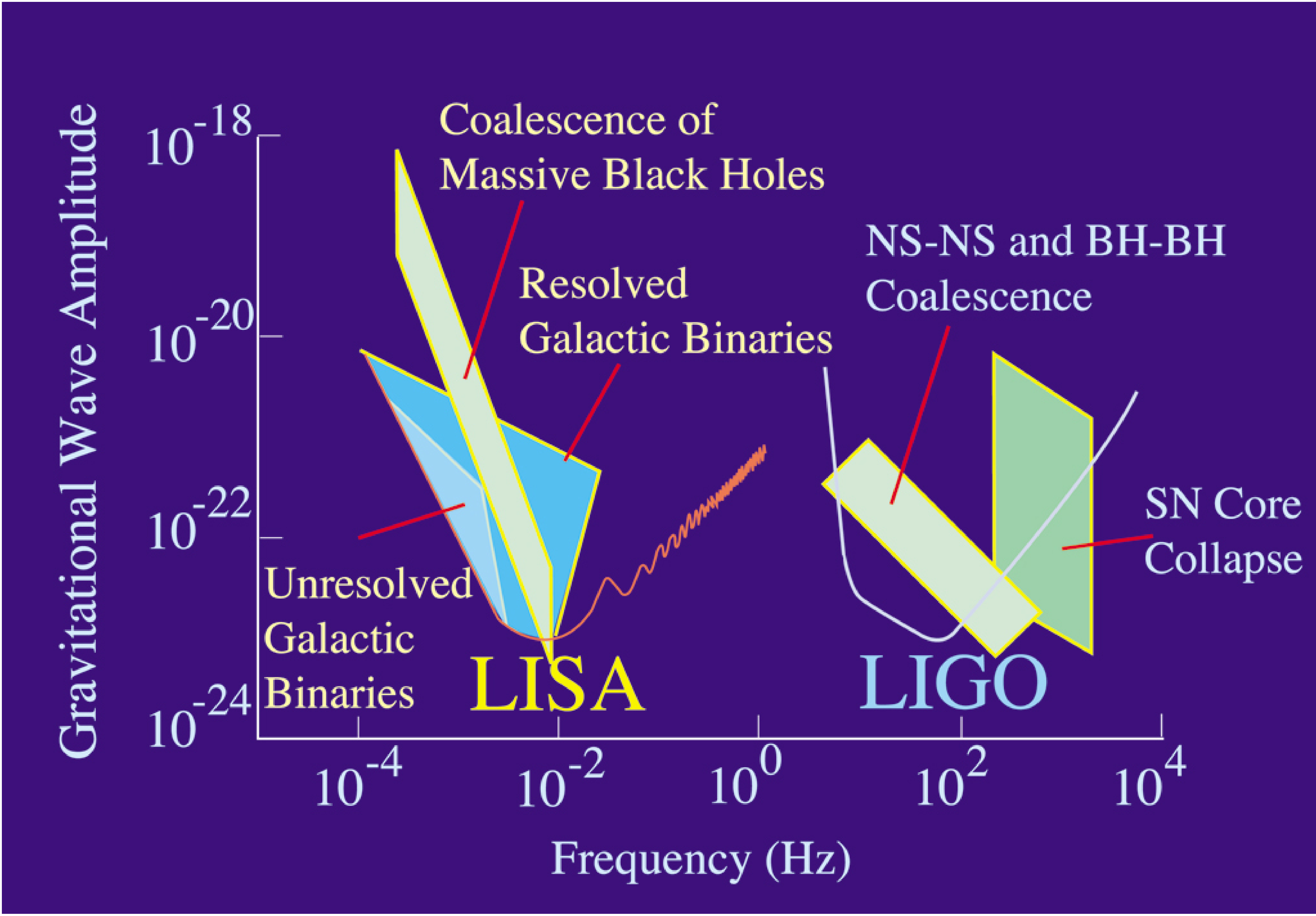
Coalescence of
Massive Black Holes
Resolved
Galactic Binaries
NS-NS and BH-BH
Coalescence
SN Core
Collapse
Unresolved
Galactic
Binaries
LISA
LIGO
Gravitational Wave Amplitude
10^-18
10^-20
10^-22
10^-24
10^-4
10^-2
10^0
10^2
10^4
Frequency (Hz)

LISA sensitivity and Black Hole science

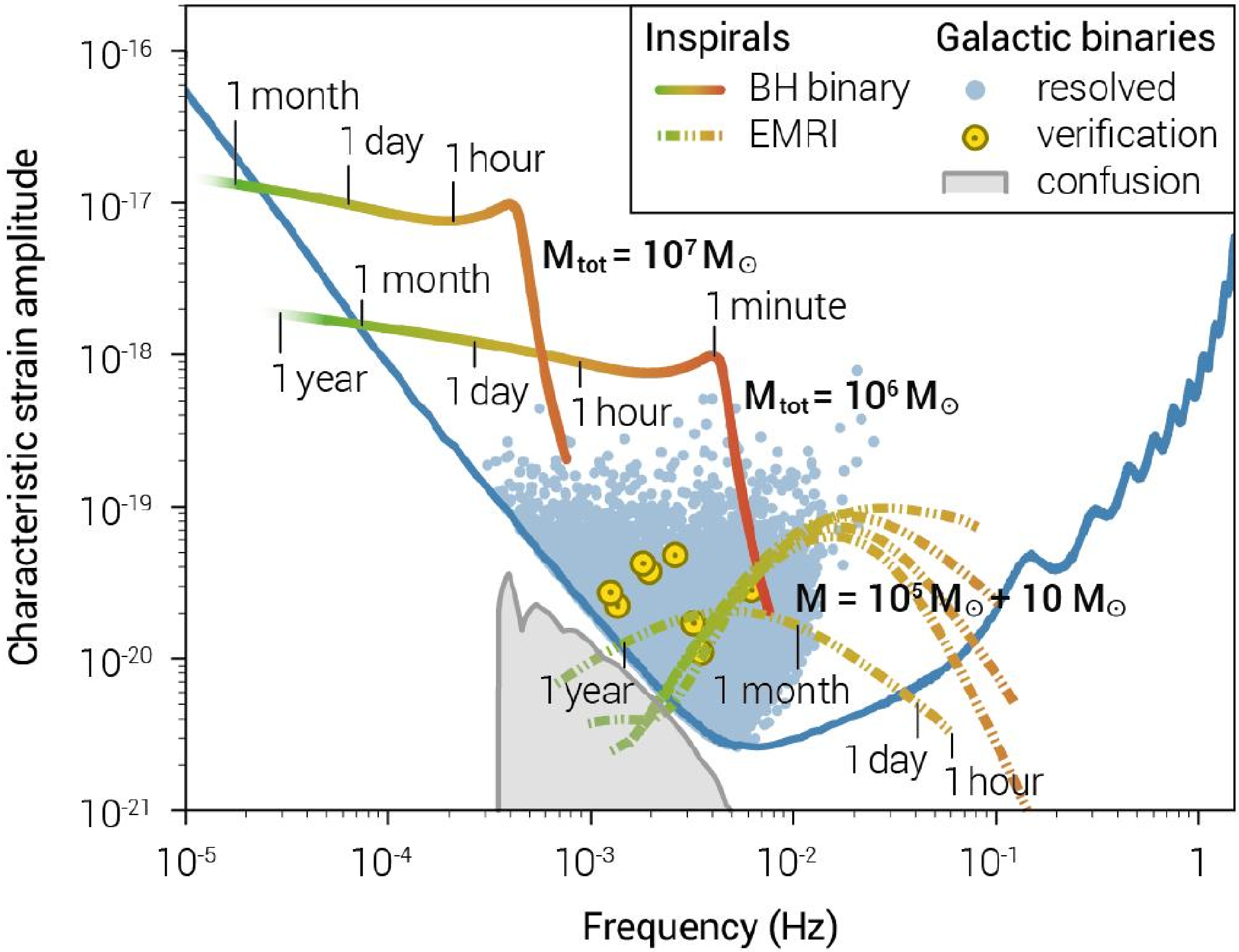

LISA: 1st LIGO event "predicted" 10 years in advance

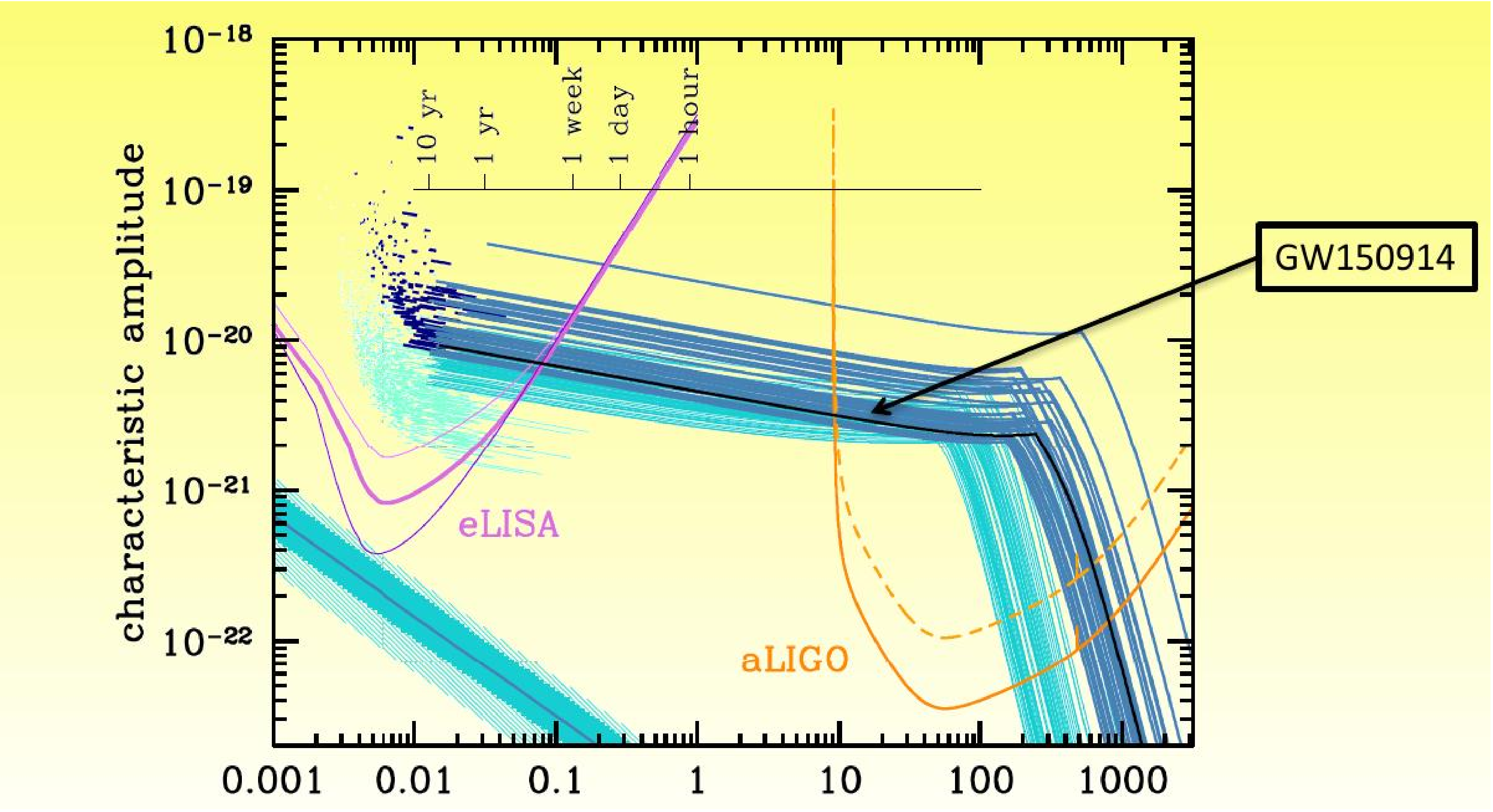

Frequency (from Sesana 2016)

Black Hole Astronomy by 2030

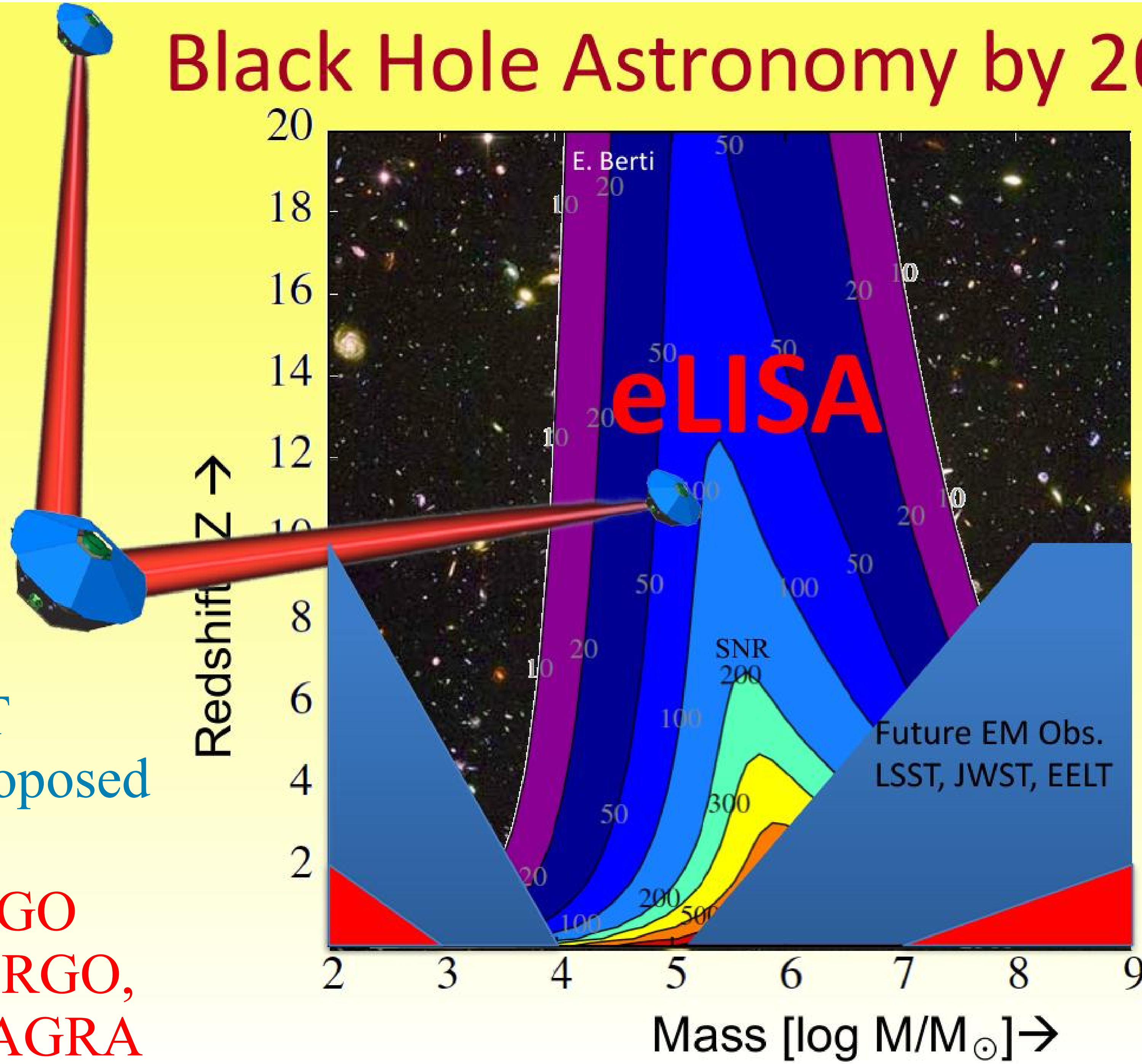

ET proposed

LIGO VIRGO, KAGRA

SKA, Pulsar Timing

LISA PATHFINDER (ESA MISSION)

Launch: 3 December 2015 - End mission: 18 July 2017

- LISA Pathfinder is the first step in the observation of gravitational waves from space
- LISA Pathfinder provides us with:
  - A better understanding of the physics of the forces acting on a free-falling test mass
  - Industrial experience in the development, manufacture, and testing of technologies required for GW detection
  - Data analysis algorithms and tools dedicated to the analysis of the system as a whole
  - Essential experience in the commissioning of a LISA-like mission
- LPF essentially shrinks one arm of LISA from ~million km down to ~40cm
  - Giving up the sensitivity to gravitational waves
  - Maintaining the instrument noise which could dominate the GW signal

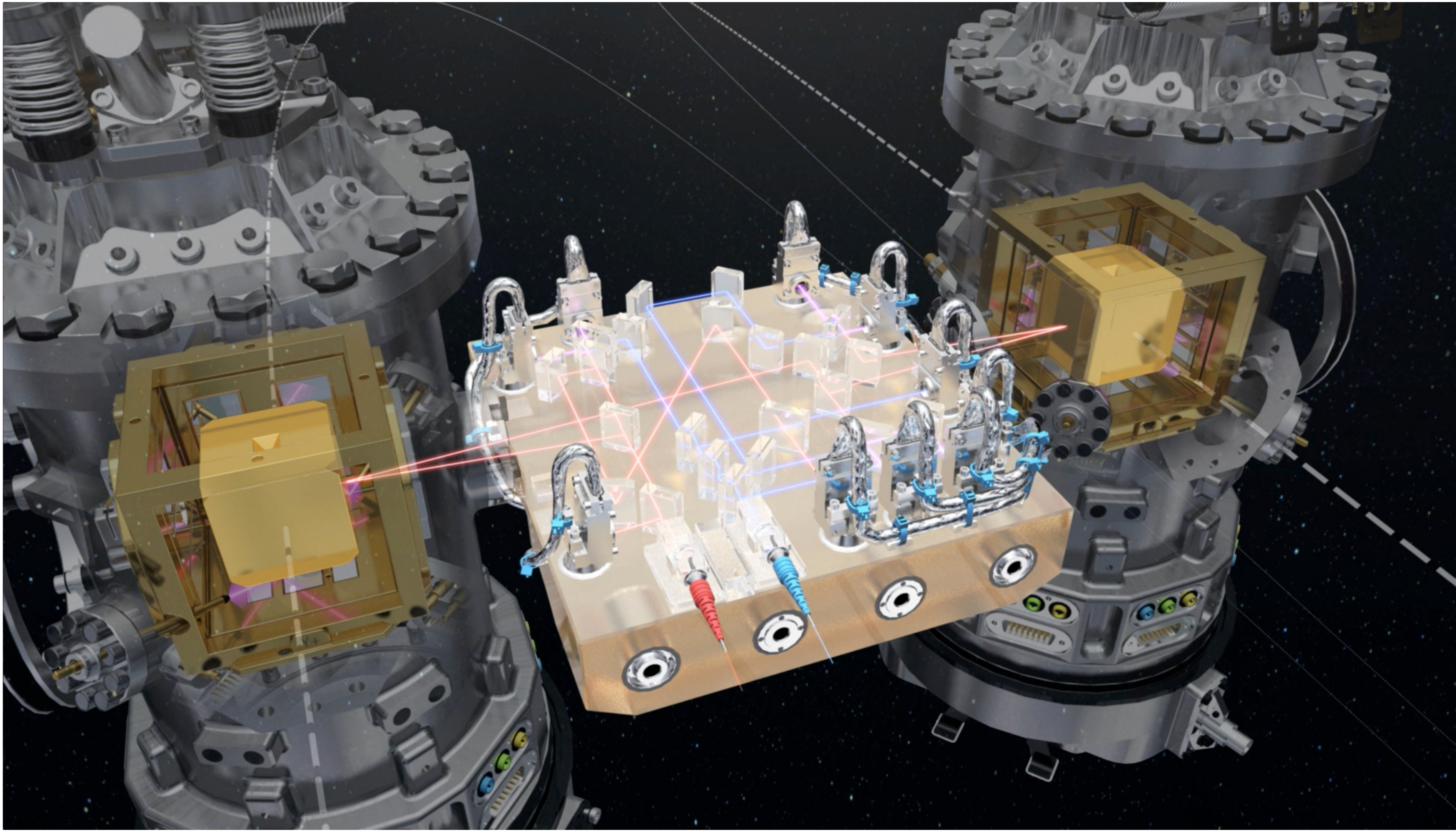

Floating test masses: 46 mm gold-platinum cubes

Launch of LISA Pathfinder on 3 December 2015

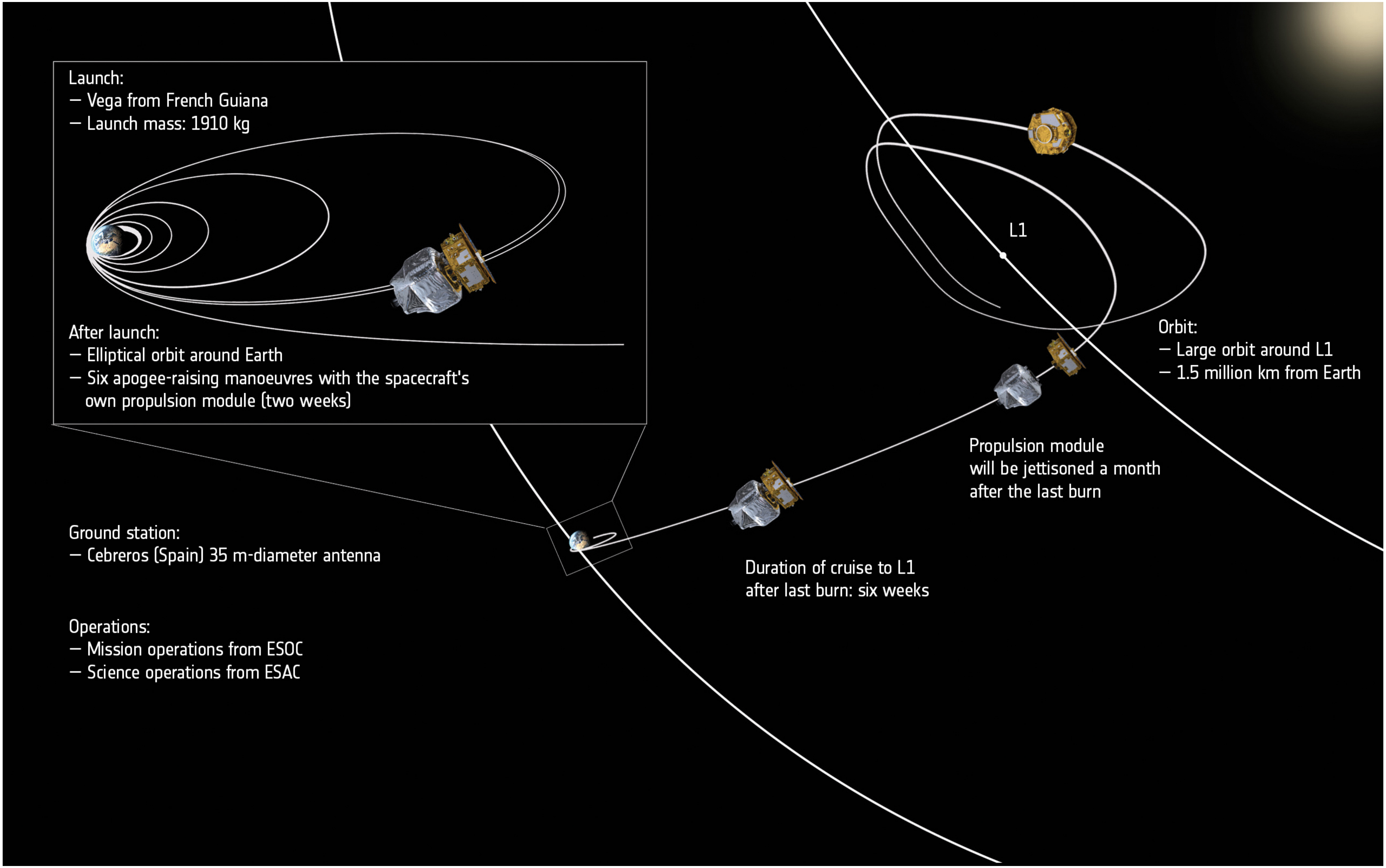

Launch:
— Vega from French Guiana
— Launch mass: 1910 kg
After launch:
— Elliptical orbit around Earth
— Six apogee-raising manoeuvres with the spacecraft's own propulsion module (two weeks)
Ground station:
— Cebreros (Spain) 35 m-diameter antenna
Operations:
— Mission operations from ESOC
— Science operations from ESAC
L1
Orbit:
— Large orbit around L1
— 1.5 million km from Earth
Propulsion module will be jettisoned a month after the last burn
Duration of cruise to L1 after last burn: six weeks

➔ LISA PATHFINDER EXCEEDS EXPECTATIONS

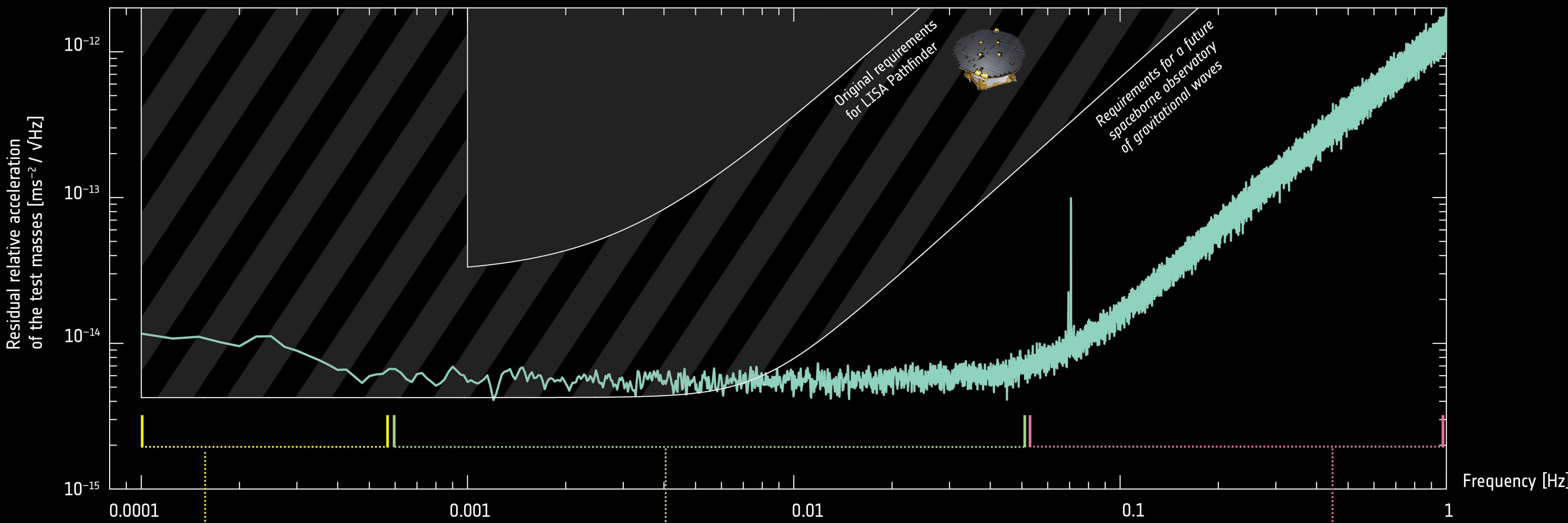

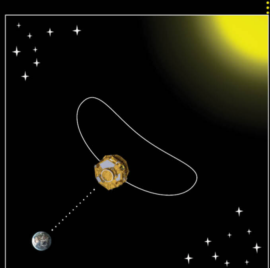

Centrifugal force

The rotation of the spacecraft required to keep the solar array pointed at the Sun and the antenna pointed towards Earth, coupled with the noise of the startrackers produces a noisy centrifugal force on the test masses. This noise term has been subtracted, and the source of the residual noise after subtraction is still being investigated.

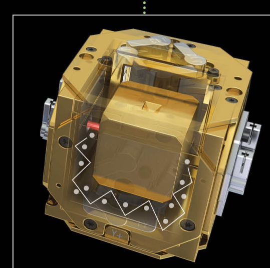

Gas damping

Inside their housings, the test masses collide with some of the few gas molecules still present. This noise term becomes smaller with time, as more gas molecules are vented to space.

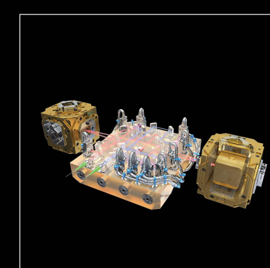

Sensing noise

The sensing noise of the optical metrology system used to monitor the position and orientation of the test masses, at a level of 35 fm / √Hz, has already surpassed the level of precision required by a future gravitational-wave observatory by a factor of more than 100.

www.esa.int

Spacecraft: ESA/ATG medialab; data: ESA/LISA Pathfinder Collaboration

European Space Agency

LISA Sensitivity with current Pathfinder performance

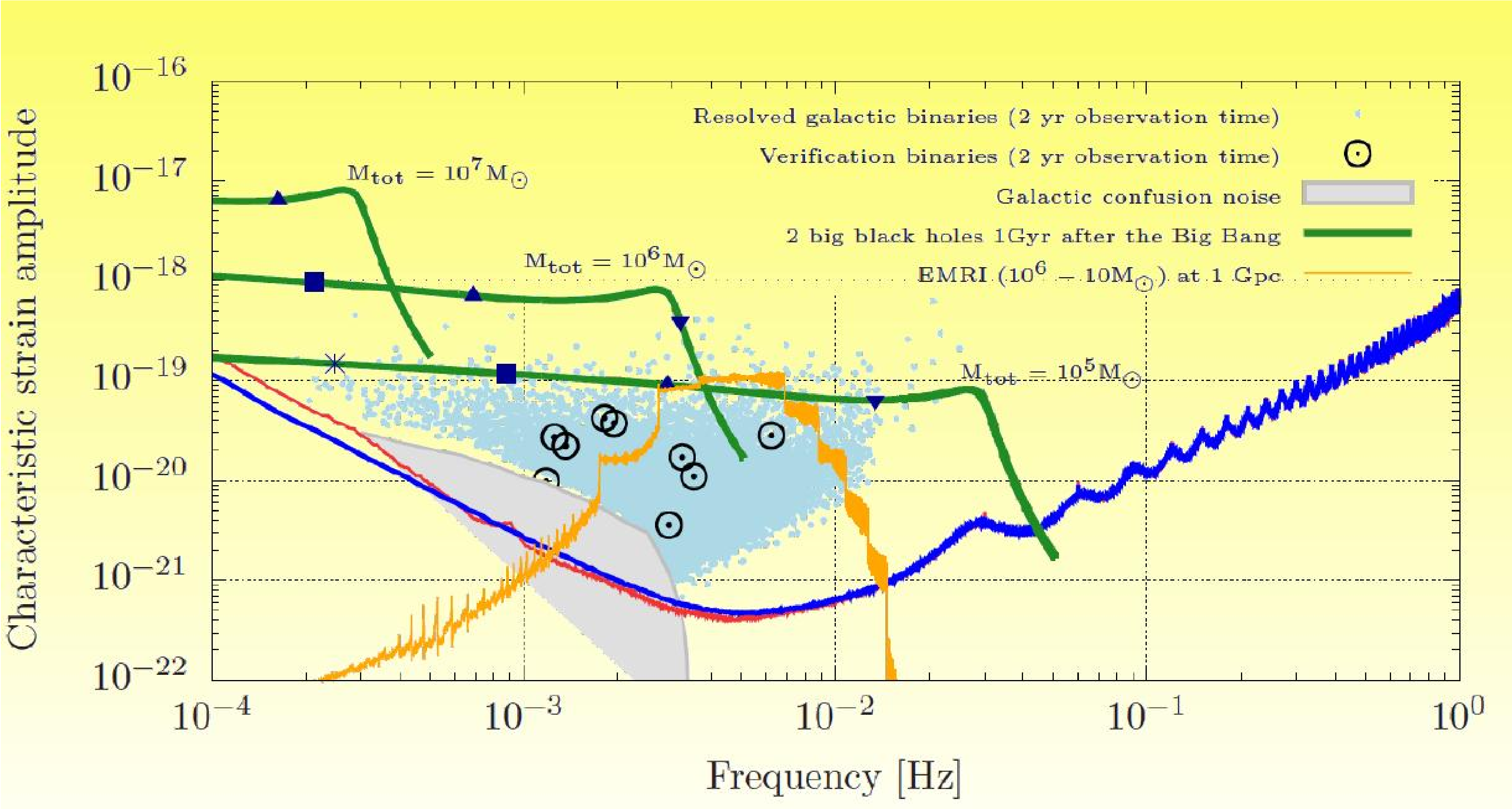

* 1 year; ■ 1 month; ▲ 1 day; ▼ 1 hour before coalescence

Black Hole merger for above noise for LISA:

10^5 Solar Mass BH binary merger at z=5

In red: Pathfinder instrumental noise

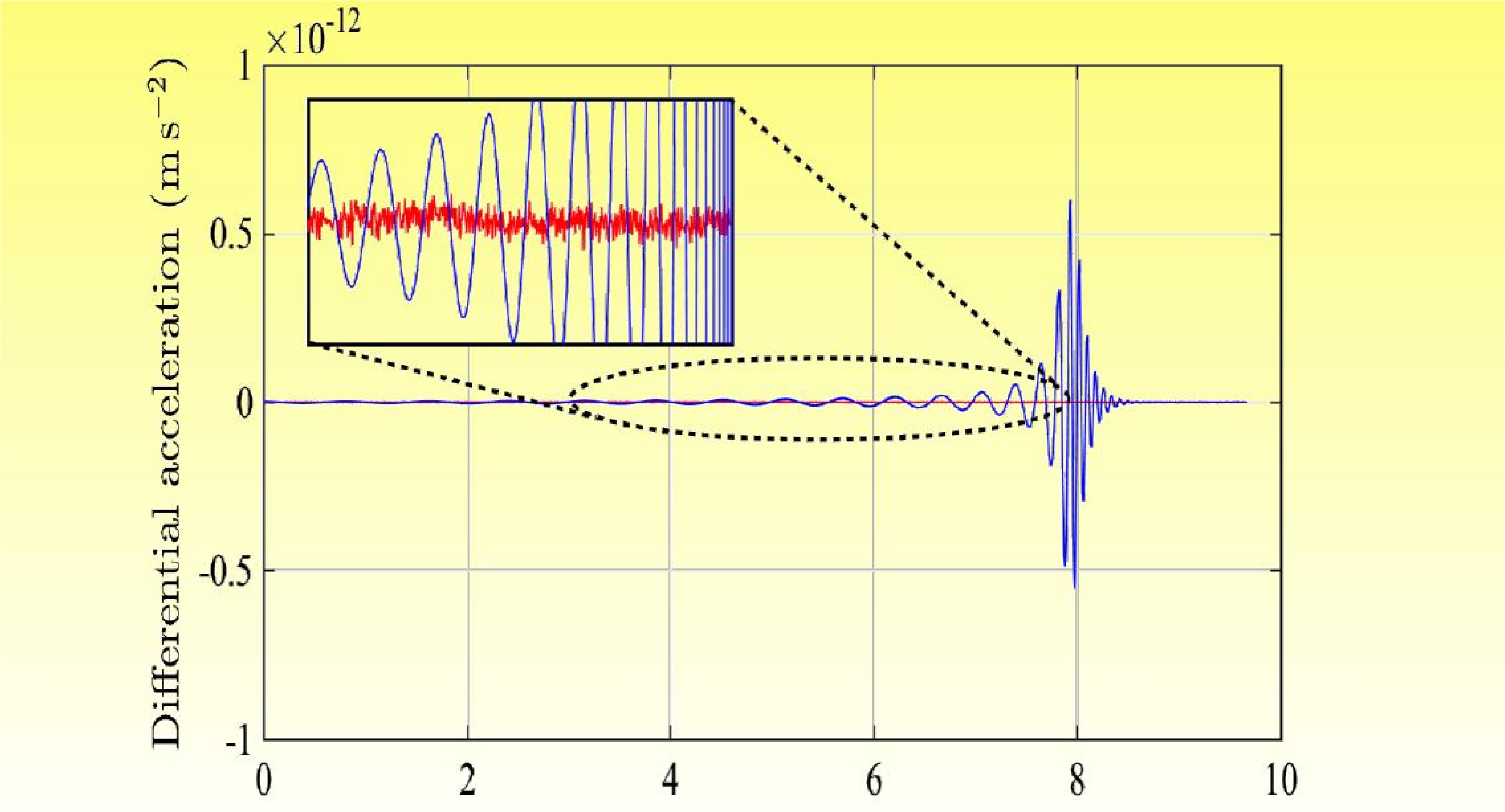

Time (in hours) (Petiteau 2016)

Within ESA’s Cosmic Vision plan:

The Gravitational Universe was identified in 2013 as the Theme for the L3 Large-class mission

On 20 June 2017 LISA has been selected as the third (L3) Large-class mission in ESA’s Science programme. Following this selection the mission design and costing can be completed and will be then proposed for “adoption” (early 2020s) before construction begins.

Currently launch is foreseen for 2034, however could be also anticipated.

The LISA Consortium includes also NASA participation.

GRAVITATIONAL WAVE ASTRONOMY HAS STARTED